Optimal Design of Negative Emission Hybrid Renewable Energy Systems with Biochar Production[1]

Lanyu Li[a], Zhiyi Yao[a], Siming You[b], Chi-Hwa Wang[a], Clive Chong[c], Xiaonan Wang[a,*]

[a]Department of Chemical and Biomolecular Engineering, National University of Singapore, Singapore, 117585

[b]School of Engineering, University of Glasgow, UK, G12 8QQ

[c]Technoponics Pte Ltd, 2G Neo Tiew Lane 1, Singapore, 719059

** Email: chewxia@nus.edu.sg Tel: +65 6601 6221*

ABSTRACT

To tackle the increasing global energy demand the climate change problem, the integration of renewable energy and negative emission technologies is a promising solution. In this work, a novel concept called "negative emission hybrid renewable energy system" is proposed for the first time. It is a hybrid solar-wind-biomass renewable energy system with biochar production, which could potentially provide energy generation, carbon sequestration, and waste treatment services within one system. The optimization and the conflicting economic and environmental trade-off of such system has not yet been fully investigated in the literature. To fill the research gap, this paper aims to propose a stochastic multi-objective decision-support framework to identify optimal design of the energy mix and discuss the economic and environmental feasibilities of a negative emission hybrid renewable energy system. This approach maximizes energy output and minimizes greenhouse gas emissions by the optimal sizing of the solar, wind, combustion, gasification, pyrolysis, and energy storage components in the system. A case study on Carabao Island in the Philippines, which is representative of an island-mode energy system, is conducted based on the aim of achieving net-zero emission for the whole island. For the island with a population of 10,881 people and an area of 22.05 km^2, the proposed optimal system have significant negative emission capability and promising profitability with a carbon sequestration potential of 2795 kg $CO_{2\text{-eq}}$/day and a predicted daily profit of 455 US$/day.

Keywords: Biochar; Gasification; Hybrid renewable energy system (HRES); Optimization; Pyrolysis; Negative emission technologies (NETs)

[1] The short version of the paper was presented at ICAE2018, Aug 22-25, Hong Kong. This paper is a substantial extension of the short version of the conference paper.

1 INTRODUCTION

As a proactive measure to reduce the risk and impacts of climate change, the Paris Agreement targets to hold the increase of the global average temperature to well below 2°C compared with pre-industrial levels by the end of this century and pursues efforts to limit it to 1.5°C [1]. It can be translated into a target of limiting the atmospheric greenhouse gas concentration to a range of 430-480 parts per million (ppm) equivalent carbon dioxide emissions ($CO_{2\text{-eq}}$) [2]. The carbon dioxide emission generated from fossil fuel combustion and industrial processes accounted for 65% of global greenhouse gas emission in 2010, and the energy sector was found to be the largest source for greenhouse gas emission [3]. Although the penetration of renewable energies in the energy systems grows steadily in recent years [4], the energy sector is still a major contributor to global greenhouse gas emission [5] due to the continuous growth of energy demand and the high reliance on fossil fuels [6]. In the most recent assessment report published by IPCC, 65% of the carbon budget in keeping the 2°C target has been consumed [7]. With an increase of 1.4% after three years' plateau, the global energy-related greenhouse gas emission (GHGe) reached its highest value of 32.5 gigatonnes (Gt) in 2017 [8]. Therefore, substantial emission reductions in the energy system would be needed to meet the targets of the Paris Agreement [9].

Under this context, there is an on-going transition of the energy system towards sustainable, low-carbon, and affordable electricity derived from renewable energies. Renewable energy technologies, especially those utilizing solar, wind, and biomass resources, have been widely studied and developed as an alternative to fossil fuels for energy production. However, considering the rate of greenhouse gas emissions, the growth of energy demand, as well as the short of efficiency to promote emission mitigation strategies so far, it is challenging to meet Paris Agreement targets without Negative emission technologies (NETs) [10]. NETs are technologies that remove greenhouse gas from the atmosphere [11]. As summarized in Table 1, various NETs have been proposed, including afforestation and reforestation (AR), soil carbon sequestration (SCS), biochar for soil amendment, bioenergy production with carbon capture and storage (BECCS), enhanced weathering (EW), direct air capture (DAC) of CO_2 from ambient air and storage, and ocean fertilization (OF) [12]. In the meanwhile, negative emission technologies (NETs) are also widely investigated in recent years along with the traditional mitigation methods such as renewable energies [13].

Table 1. Main features of the typical NETs.

NETs	Maximum Potential CO_2 removal capacity (Gt-$CO_{2\text{-}}$	Technical Readiness level (TRL) [14]	Maximum land requirement (Mha) [15]	Water requirement (km^3/yr) [15]	Maximum energy requirement (10^{18} J/yr) [15]	Estimated cost (USD/ t-$CO_{2\text{-eq}}$.) [14]

	$_{eq}$./yr) [14,15]					
BECCS	2.4-10	4-6	380-700	720	-170	70-250
Biochar	0.7-3	4-6	40-260	0	-14 to -65	8-300
DAC	3.3-10	3-6	Little	10-300	156	40-600
EW	0.2-0.4	6-7	2-10	0.3-1.5	46	60-200 [16]
FR	1.5-3	6-7	320-970	370-1040	Little	20-100
OF	0-1	1-4				71-330 [17]

Among the NETs, carbon sequestration by biochar is one of the most attractive options with high technical readiness, good carbon abatement potential, and moderate cost [18]. As a carbon-rich solid residue derived from gasification and pyrolysis, biochar has been recognized as an effective carbon abatement tool upon its application to soil. Since CO_2 is absorbed during plant growth, there is a net zero emission of CO_2 when biomass is combusted. Through converting biomass into biochar for soil application, a significant amount of carbon could be sequestrated, leading to a net removal of CO_2 from the atmosphere. Additionally, biochar could also increase soil organic matter [19], microbial activity [20], water retention, and crop yields [21], while decrease fertilizer needs, soil greenhouse gas emissions, nutrient leaching, erosion, pollutant bioavailability and pollutant mobility [22–24], leading to an overall effect of indirect carbon abatement.

To produce both biochar and electricity, two waste-to-energy technologies are commonly applied: gasification and pyrolysis. Gasification could convert a carbonaceous feedstock into heat, biochar, and producer gas, which mainly consists of CO_2, CO, H_2, CH_4, and N_2 in a high-temperature, oxygen-insufficient environment [25]. In the pyrolysis process, organic material decomposes mainly into pyrolytic gas, pyrolytic oil, and biochar in the absence of oxygen [26]. In these processes, heat contained in the gas phase can be used to generate electricity. When more biochar is produced, less energy is contained in the gas phase, leading to a lower electricity generation rate and vice versa. As the amount of electricity and biochar productions are negatively correlated, there is a trade-off between them, which further leads to a trade-off between economic profit and carbon sequestration. Another thermal chemical process, combustion, can be employed to increase the energy utilization efficiency of the biomass. Complementary power generation methods can also be incorporated to target higher carbon sequestration goals while meeting the electricity demand in a system level. As solar and wind resources are abundant, endless, and accessible with no cost [27], solar photovoltaic (PV) and wind energy are recognized as two promising and popular choices for renewable power generation.

Therefore, it is important to select the most economical pathways and sizes of the system components to maximize the economic and environmental performance of the NEHRES while meeting the power supply requirements.

In order to effectively design a NEHRES that possesses carbon sequestration and cost-effectiveness while ensuring reliable energy supply, optimization methods can be used. In this study, we aim to propose a decision-support framework for the optimal design of a NEHRES. A case study on a standalone rural island where solar, wind and biomass resources are available will be conducted to demonstrate the proposed framework and the feasibility of a negative emission hybrid renewable energy system.

The remaining part of the paper is organized as follows. Section 2 presents a brief and general review of the state-of-the-art optimization methods for the design of renewable energy systems and the contribution of this work to the research field. A proposed stochastic multi-objective optimization framework for the design of the NEHRES is detailed in Section 3. The background of the case study will be introduced in Section 4. The results and discussion of the case study will be provided in Section 5 and the conclusions drawn in Section 6.

2 LITERATURE REVIEW

A problem of renewable energy is that it is highly dependent on the environment, which can lead to an intermittent and fluctuating power generation. This problem poses challenges for the energy system to provide a stable and reliable electricity supply. Two solutions to this problem, energy storage and HRES, have been proposed by the researchers. An energy storage system, such as a battery bank, can be used to store excess electricity for later use. It is currently a necessary component for renewable energy applications to ensure the reliability of the energy supply [29]. Further, the use of different energy sources in a HRES, can not only provide more flexible, reliable, and efficient electricity supply than a single renewable energy source but also reduce energy storage requirements [30].

The design of a HERS is more complicated than a single renewable technology [31]. Since the financial investment, system operation, and supply-demand balance are dependent on the capacity of the system components of the HRES, how to achieve optimal sizing of the components in the HRES is a critical problem. Many studies have been conducted to investigate the optimization and sizing of HRES. Cost reduction, system reliability improvement, and environmental performance are typical optimization criteria. The optimization methods applied to the design of HRES can be categorized into conventional optimization methods (e.g. linear and non-linear programming, dynamic programming, multi-objective optimization, stochastic programming, and software such as HOMER, HYBRID2, HYBRIDS, RET Screen, TRNSYS and IHOGA [32]), artificial-intelligence-based techniques (e.g. ant colony, genetic algorithm, knowledge-based system, and particle swarm optimization), and hybrid techniques [33]. A detailed list of the recent research work on the optimization of HRES containing solar, wind, and biomass components is

provided in Table 2.

Table 2. Recent research work on the optimization of solar, wind, and biomass integrated HRES.

Authors and References	Renewable energy sources	NETs	Methods	Objective functions
Pérez-Uresti et al., 2019 [28]	Solar, wind, and biomass	No	Superstructure and mixed-integer nonlinear programming	Total annual cost
Meng et al., 2019 [34]	Solar, wind, biomass, and tidal	No	Multi-objective stochastic chance constrained programming	Economic optimality, environmental friendliness, and energy exploitation and utilization efficiency
Gonzalez et al., 2018 [35]	Solar, wind, and biomass	No	Genetic algorithm-based multi-objective optimization	Economic and environmental impact are minimized
Ahmad et al., 2018 [36]	Solar, wind, and biomass	No	Homer Pro	Levelized cost of energy
Hocine et al., 2018 [37]	Solar, wind, biomass, and tidal	No	A hybrid uncertainty goal programming approach proposed	Investment costs, operating and maintenance costs, primary energy saving, realization time, sustainability of climate change, and job creation
Martín and Grossmann, 2018 [38]	Solar, wind, and biomass	No	Mixed-integer linear programming Surrogate models	Production cost
Chauhan and Saini, 2017 [39]	Solar, wind, micro-hydro, and biomass	No	Integer linear programming Demand response	Total annualized cost
Chauhan and Saini, 2016 [40]	Solar, wind, micro-hydro, and biomass	No	Techno-economic Load shifting based demand-side management strategy has been suggested	Net present cost
Singh et al., 2016 [41]	Solar, wind, and biomass	No	Evolutionary algorithms	Annualized system cost

Based on the literature review, it is found that few studies have looked into the incorporation of gasification and pyrolysis processes in the HRES, although a lot of research work has been carried out for solar-wind-biomass-integrated HRES. Moreover, there is a gap in understanding potential trade-offs between conflicting economic and environmental targets using a whole-system modeling and optimization approach not only for pyrolysis and gasification processes [42], but also for the NEHRES that contain these technologies.

Therefore, the motivation of this work is to fill the aforementioned research gaps and identify potential renewable mix that could possibly address the energy, climate change, and waste management issues simultaneously. The contributions of this paper are summarized as follows:

- Proposes a superstructure of biochar-integrated HRES that could achieve the goals of energy generation, carbon sequestration, and waste treatment services, as well as a novel concept of negative emission hybrid renewable energy systems for the first time.
- Carries out detailed modeling of different components in the NEHRES and employed data-driven models to depict the gasification and pyrolysis processes.
- Develops a multi-objective stochastic decision-support framework for the optimal design of a NEHRES considering economic and environmental criteria.
- Investigates the trade-off between carbon sequestration and economic benefit for a NEHRES, and demonstrates the system design and operation, sensitivity and robustness of the system subject to different scenarios, and the potential application of the NEHRES to different scales.

3 METHODOLOGY

The proposed layout of the NEHRES is shown in Figure 1. In the system, gasification and pyrolysis are the key contributors to negative emission through biochar production and application, while solar PV, wind, and biomass combustion technologies serve as main sources for electricity supply. The producer gas undergoes several processes and enters the turbine for electricity generation. When gasification and pyrolysis processes are chosen for biomass conversion, the liquid and solid products undergo the separation process to obtained biochar, which would be finally applied for carbon sequestration and soil amendment. Electricity generated from the biomass, solar, and wind resources is controlled and regulated with an energy storage system to adapt to the load. The size of the biomass conversion technologies is determined by the capacity of the individual equipment while the PV and wind systems are dealt with as modular systems, meaning the size of the PV and wind systems is determined by the number of modules installed. Generation, storage, and discharge of electricity are also determined according to a control strategy that optimizes the objectives in the model.

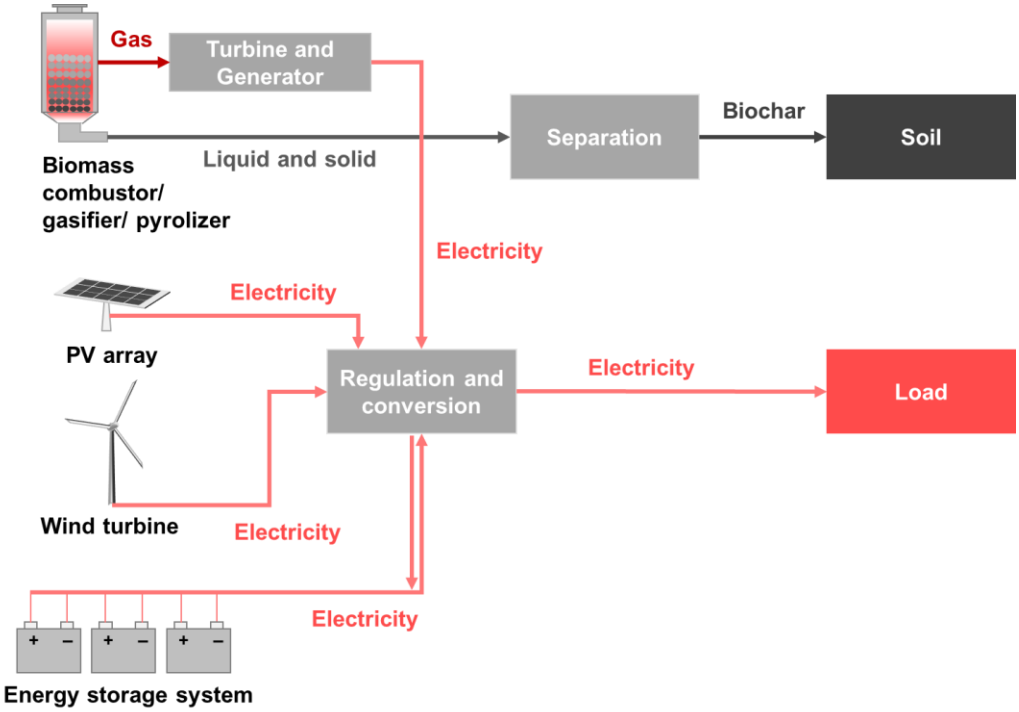

Figure 1. The schematic diagram of NEHRES.

Based on the NEHRES scheme, the decision-support framework for the sizing of the NEHRES is demonstrated in Figure 2. The framework includes data collection and analysis, system modeling, optimization, and post-optimality analysis.

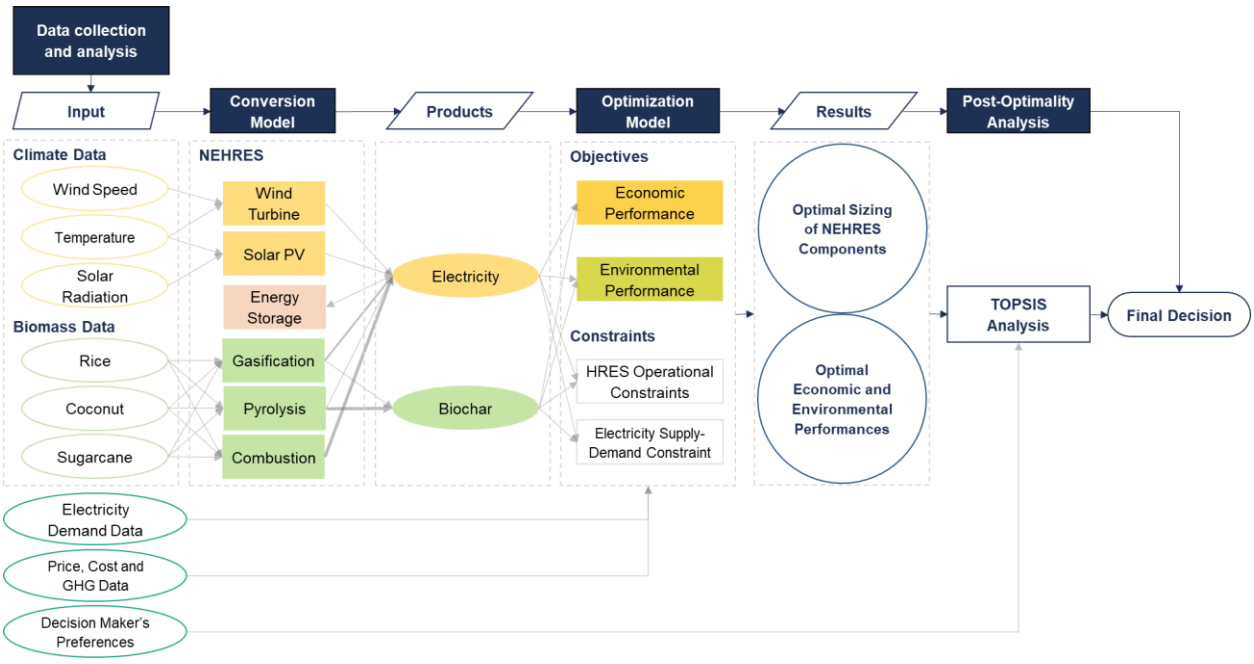

Figure 2. The decision-support framework for the design of the NEHRES.

The first step in the proposed method is data compilation regarding local renewable energy resources which are usually featured by temporal fluctuations or seasonality for the stand-alone system. Then the input data are fed into the energy conversion models. In this case, wind speed and temperature are required to calculate the maximum potential of power generated from the wind. Solar radiation and temperature are used to estimate the maximum possible power generation derived from solar energy. The availability of biomass waste is utilized to assess the maximum production of electricity and biochar from different thermochemical processes. The maximum resource availability is used as the resource constraints in the optimization process. The actual electricity and biochar production is calculated by the conversion model using the number of wind turbines, solar panels, and the feeding rates of biomass as input. These input values are also the decision variables that determine the size of each component of the NEHRES.

The outputs of the two major products of the NEHRES (i.e. electricity and biochar), the electricity demand data, the price and cost data, and the life-cycle greenhouse gas emission data serve as the inputs for the assessment of the economic and environmental performances of the system in the optimization model. Optimization solvers can be used to obtain the optimal system design and the corresponding economic and environmental performances.

Finally, the optimal decision variables can be returned, and the results of the optimal sizing of each component and the corresponding economic and environmental performances of the NEHRES are obtained. TOPSIS analysis is used as a post-optimality analysis method to rank the Pareto solution based on the decision maker's preferences. The results obtained from TOPSIS analysis can be used to assist the final decision making.

Details about the conversion and optimization models as well as the post-optimality analysis method are provided in the following subsections. The process of data collection and analysis is introduced in Section 3.1. The models of the components in the NEHRES is presented in Section 3.2. The optimization model for the design of NEHRES is shown in Section 3.3. The post-optimality analysis method for multi-objective optimization is described in Section 3.4.

3.1 DATA COLLECTION AND ANALYSIS

Data collection and analysis is the first step of system modeling. The electricity demand profile, the meteorological data, the biomass availability, unit capital and operating costs of the elements, and prices of electricity and biochar are needed to determine the optimum sizing of a hybrid renewable energy system. The electricity demand, the meteorological data, and the biomass availability data are obtained as time-series data on a daily (24-hour) basis. Linear interpolation is used to fill the gap of missing data in the time series. The costs and prices for the elements and processes as well as the interest rate can be obtained based on the local rates or the global average at the current year. By assuming that the climate pattern remains unchanged for a specific location, the average value of the meteorological data from the previous years is used to represent the yearly meteorological data throughout the lifespan of the NEHRES. The assumption of a similar pattern in the future years is also used to predict the value of other parameters throughout the lifespan of the NEHRES.

3.2 SYSTEM MODELING

The models for biomass conversion (combustion, gasification, and pyrolysis), solar energy conversion, wind energy conversion, and energy storage are illustrated in this section.

3.2.1 Bioenergy conversion

In this study, three different mathematical models were adapted to predict carbon sequestration potential and energy performance of combustion, gasification and pyrolysis process, respectively. For the combustion process, biomass feedstock is totally burnt into ashes while producing H_2O and CO_2. With the same biomass feedstock, combustion generally generates the largest amount of electricity with no biochar production, while pyrolysis produces the largest amount of biochar but least electricity, and gasification yields a moderate amount of electricity and biochar. Compositions (Y_j) and higher heating value (*HHV*) of the feedstock are two major features for the three processes. As model inputs, features of the feedstock in each process are calculated by Eq. (1)-(2).

$$Y_{j,p} = \frac{\sum_i F_{i,p} \cdot Y_{j,i}}{\sum_i F_{i,p}} \tag{1}$$

$$HHV_p = \frac{\sum_i F_{i,p} \cdot HHV_i}{\sum_i F_{i,p}} \quad (2)$$

where $Y_{j,p}$ is the mass fraction of chemical composition j in process p, $F_{i,p}$ is the mass flowrate of each type of biomass i in process p, $Y_{j,i}$ is the amount of composition j in biomass i, HHV_p is the higher heating value of feedstock in process p, and HHV_i is the higher heating value of biomass i.

3.2.1.1 Combustion

In the combustion model, the input variables are the mass flowrate and higher heating value of feedstock fed into the combustion process. It is assumed the total energy contained in the feedstock is consumed to generate electricity in the combustion process. The only output of the combustion model is electrical power P_c, which is calculated as:

$$P_c = \frac{HHV_c \times eff_c \times F_c}{3.6} \quad (3)$$

where HHV_c is the higher heating value of feedstock in the combustion process, eff_c is the electrical efficiency of an incineration plant (the ratio of electricity output to the energy of feedstock), and F_c is the mass flowrate of total biomass waste.

3.2.1.2 Gasification

For the gasification process, a machine learning model based on artificial neural networks (ANN) [43] is adapted to predict the composition and production rate of both producer gas and biochar. This is a type of data-driven method which has various advantages. For one thing, when the first-principle model of a system is unknown, data-driven methods such as machine learning can be used to build up a model to describe the relation of the input and output variables based on the available inputs and outputs information. For another, data-driven models (e.g. ANN) can potentially reduce the computational cost and fasten the optimization process compared with a first-principle model, which may consist of a series of differential equations.

The gasification process in this study is simulated using five ANN models, one for each gas output (CO, CO_2, H_2, CH_4, and total gas yield). Details about the ANN models and parameters can be found in the Supplementary Information.

The electrical power P is generated from burning the producer gas in the internal combustion (IC) engine, which is calculated by the following equation:

$$P = \frac{HHV \times eff_{thermal} \times eff_{WtoE} \times F}{3.6} \quad (4)$$

where HHV is the higher heating value of biomass fed into the process, $eff_{thermal}$ is the thermal efficiency of IC engine (the efficiency of converting the energy of feedstock to mechanical work), eff_{WtoE} is the efficiency of converting mechanical work to electricity, and F is the mass flowrate of biomass fed into the process.

The total amount of fixed carbon $M(C)_g$ derived from gasification is calculated based on mass balance:

$$M(C)_{gasification} = F_{g,feed} \cdot Y_C - Y_{gas} \cdot F_{g,gas} \cdot \rho_{gas} \cdot (\frac{Y_{CO} \cdot M_C}{M_{CO}} + \frac{Y_{CO2} \cdot M_C}{M_{CO2}} + \frac{Y_{CH4} \cdot M_C}{M_{CH4}}) \quad (5)$$

where Y_c is the mass fraction of carbon in feedstock, Y_{gas} is the producer gas yield predicted by the model, ρ_{gas} is the density of producer gas, Y_{CO}, Y_{CO2}, and Y_{CH4} are the mass fraction of CO, CO_2, and CH_4 in the producer gas, respectively, and M_{CO}, M_{CO2}, M_{CH4}, and M_C are the molecular weights of CO, CO_2, CH_4, and carbon, respectively.

3.2.1.3 Pyrolysis

In the pyrolysis process, organic material decomposes mainly into pyrolytic gas, pyrolytic oil, and biochar in the absence of oxygen. This work adapted an empirical model of biomass pyrolysis to predict the production of biochar as well as gaseous and liquid biofuels [44]. The model inputs include peak pyrolysis temperature T_p, and the mass fraction of C, O, H and lignin on dry-ash-free (DAF) basis. The empirical correlations to calculate the yields of different products are summarized the Supplementary Information.

Similar to the gasification model, the outputs for the pyrolysis model include electrical power and the total amount of fixed carbon. Pyrolytic gas is also burnt in the internal combustion engine to produce electrical power, which could be calculated using Eq. (4). On the other hand, the total amount of fixed carbon in the biochar could be calculated using the following equation:

$$M(C)_{pyrolysis} = F_{p,feed} \times Y_{char} \times Y_{C(char)} \quad (6)$$

where F_p (kg/h) is the mass flowrate of total biomass waste fed to the pyrolysis process, Y_{char} is the yield of biochar, and $Y_{C(char)}$ is the mass fraction of fixed carbon contained in biochar.

For the biochar generated by the gasification and pyrolysis processes, the carbon sequestration performance of biochar can also be evaluated using a carbon stability factor ($W_{CO2/C}$) [45], which indicates the amount of CO_2 sequestrated for each unit of fixed carbon. Therefore, it ranges from zero to 3.66 g CO2eq/g biochar-C. It is calculated by:

$$W_{CO_2/C} = 3.66 \cdot (1 - e^{t_{1/2} \cdot \ln(0.5)/TH}) \quad (7)$$

where $t_{1/2}$ is the half-life of biochar in soil and TH is the time horizon of interest.

3.2.2 Solar energy conversion

Generally, the electrical parameters including the maximum power current and voltage and the maximum power points measured under the standard rating conditions (SRC) (1 kW/m^2 irradiance, 25 °C cell temperature) are provided in the datasheet of the photovoltaic modules [46]. However, the power output can be influenced by the incident solar radiation, cell temperature, solar incidence angle and load resistance in real operation [47]. Two commonly used models, the single and double diode models, can be used to describe the actual behavior of the solar generator systems [48].

Among the two models, the single diode model is more widely used due to its simplicity and competent accuracy [49]. The formulation of the single diode model is shown in Eq. (8)-(9).

$$I_l - I_d\{\exp[\varepsilon \cdot (U + R_{se} \cdot I) - 1\} - \frac{U - R_{se} \cdot I}{R_{sh}} = I \tag{8}$$

$$\varepsilon = \frac{q}{N_s n_I k T_c} \tag{9}$$

where I_l, I_d, and I are the light-generated current, diode saturation current, and the output current in the cell, respective. U is the voltage of the cell, R_{se} is the series resistance, R_{sh} the shunt resistance, ε is the modified ideality factor, q is the elementary charge (1.602×10^{-19} C), and N_s is the number of cells in series, n_I is the diode ideality factor, k is the Boltzmann's constant (1.381×10^{-23} J/K), and T_c is the cell temperature.

The existing methods used to solve the single diode model can be categorized into the analytical method, analytical plus optimization method, and optimization method [46]. In this study, the analytical plus optimization method proposed by De Soto et al. is used [47]. The power generated by the photovoltaic system (P_s) can be calculated by:

$$P_s = U \cdot I \tag{10}$$

3.2.3 Wind energy conversion

The wind power generation depends on the mechanical power captured by a wind turbine. It can be described by a wind-speed dependent piece-wise function shown in Eq. (11). There are three characteristic speeds of the wind turbine operation: the cut-in speed (v_{ci}), at which the blades of the wind turbine overcome the friction and start rotation; the rated speed (v_r), above which the wind turbine is operated at its rated power; and the cut-out speed (v_{co}), which is set to bring the blades to rest to avoid damage from strong wind. When the wind speed is less than the cut-in speed (v_{ci} = 5m/s) or larger than the cutout speed (v_{co} = 20 m/s), there will be no generation. When the wind speed is above the rated wind speed and below the cut-out wind speed, the blade pitch angle of the wind turbine would be controlled to generate a constant output power (P_r). When the rated wind speed falls in the range between the cut-in speed and cut-out speed, the power generation is affected by the air density (ρ), the wind speed (v), the swept blade area (Ar), and the coefficient of power (C_p) which is a function of λ ($\lambda = r\omega m/v$) and the blade pitch angle [50].

$$P_w = \begin{cases} 0, & v \le v_{ci} \text{ or } v \ge v_{co} \\ \frac{1}{2} \cdot \rho \cdot C_p \cdot Ar \cdot v^3, & v_{ci} \le v \le v_r \\ P_r, & v_r \le v \le v_{co} \end{cases} \tag{11}$$

3.2.4 Energy storage

The energy storage component balances the mismatch between electricity generation and consumption. Based on the characteristic of the supply-demand curve, the capacity, discharge time,

and frequency of charging and discharging requirements of the energy storage system can be determined. With such information, the technically suitable energy storage technology can be screened out from various types of existing storage options for the subsequent economic and environmental optimization. The capacity, the maximum amount of energy that can be stored, is a major design parameter for the energy storage system. To determine this value, the state of charge (SOC_t) of the energy storage system, which indicates the amount of energy storage at any time t, can be calculated by:

$$SOC_t = (\sum_{t=1}^{t} S_{in,t} \cdot \Delta t) - (\sum_{t=1}^{t} S_{out,t} \cdot \Delta t) - \frac{(1-\eta)}{2}(\sum_{t=1}^{t} S_{in,t} \cdot \Delta t) - \frac{(1-\eta)}{2}(\sum_{t=1}^{t} S_{out,t} \cdot \Delta t) \quad (12)$$

where S_{in} is the amount of energy entering the energy storage system, S_{out} is the amount of energy flowing out of the energy storage system, t is time, Δt is the length of each time interval, and η is the round-trip efficiency.

3.3 Optimization Model for the Design of NEHRES

Following the modeling of system components in Section 3.2, the optimization model for the design of NEHRES is presented in this section. As the economic and environmental performances are two critical concerns for an energy system, it is aimed to design the NEHRES by maximizing the profit and minimizing the greenhouse gas emissions with various constraints. A multi-objective optimization method can be applied for this purpose. In order to determine the optimal capacity of the energy storage system, which is dependent on the daily generation and demand profile, the assessment and optimization of the NEHRES are carried out based on a 24-hour operation. Accordingly, the two objective functions in the optimization are expressed on a daily basis, which is, in the form of the daily net cash flow (NCF) and daily greenhouse gas emissions (GHGe). The formulation of the objective functions is shown in Section 3.3.1 and 3.3.2. The constraints for the optimization is shown in Section 3.3.3. Finally, the overall stochastic optimization model is given in Section 3.3.4.

3.3.1 Economic objective: Daily Net Cash Flow

Life-cycle cost (LCC) analysis is a conventional method for the assessment of the techno-economic feasibility of a HERS. In this study, a life-cycle cost-benefit analysis is used as the basis to calculate the daily net cash flow of the system. To make the calculation consistent with the daily scope of the evaluation, the investment cost is annualized and considered as part of the fixed cost, which is further converted to a daily fixed cost (FC) by dividing the number of days under operation in a year (t_{op}). Therefore, one of the objective functions, the daily net cash flow (NCF) is calculated using the below equation:

$$NCF = -FC + (\sum_{t=0}^{23} (Revenue_t - VC_t)) \quad (13)$$

where FC is the daily fixed cost, $Revenue_t$ is the hourly revenue from the sales of the products of the NEHRES, and VC_t is the variable costs. Their values are calculated by the following equations:

$$FC = \frac{CAPEX \cdot CRF + FOM}{t_{op}} \tag{14}$$

$$CAPEX = \sum_k C_{CAPEX,k} \cdot P_{capacity,k} + C_{storage\_CAPEX\_P} \cdot S_{\max} + C_{storage\_CAPEX\_E} \cdot SOC_{\max} \tag{15}$$

$$CRF = \frac{r \cdot (1+r)^T}{(1+r)^T - 1} \tag{16}$$

$$FOM = \alpha \cdot CAPEX \tag{17}$$

$$VC_t = VOM_t + Fuel_t \tag{18}$$

$$VOM_t = (\sum_k C_{vom,k} \cdot P_{gen,k,t} \cdot \Delta t) + C_{storage} \cdot (S_{in,t} + S_{out,t}) \cdot \Delta t \tag{19}$$

$$Fuel_t = \sum_i C_{fuel,i} \cdot F_{i,p,t} \cdot \Delta t \tag{20}$$

$$Revenue_t = C_{elec} \cdot P_{sell,t} + C_{biochar} \cdot m_{biochar,t} \tag{21}$$

where *CAPEX* is the total capital investment cost of the NEHRES, *CRF* is the capital recovery factor, and *FOM* is the fixed operating and maintenance cost, which is assumed to be proportional to the capital cost by a factor of α. $C_{CAPEX,k}$ is the unit capital investment cost of the component in the NEHRES, $C_{storage\_CAPEX\_P}$ and $C_{storage\_CAPEX\_E}$ are the unit power and energy capital investment cost of the energy storage component, $P_{capacity,k}$ is the capacity of the component, S_{max} is the power capacity of the energy storage component, and SOC_{max} is the energy capacity of the energy storage component. r is the interest rate and T the lifespan of the NEHRES. VOM_t is the variable operating and maintenance cost of the NEHRES at time t. *Fuel* is the fuel cost, which refers to the cost of the biomass in this case. C_{vom} is the unit cost of the operation and maintenance of the power generation components, $C_{storage}$ is the unit cost of the operation and maintenance of the energy storage component, C_{fuel} is the unit cost of the fuel, F is the mass of biomass fed into the biomass conversion process p at time t, and Δt is the time interval which is one hour in this study. C_{elec} is the unit selling price of electricity, $P_{sell,t}$ is the amount of electricity sold at time t, $C_{biochar}$ is the unit selling price of biochar, and $m_{biochar,t}$ is the mass of biochar sold at time t.

3.3.2 Environmental objective: Daily greenhouse gas emissions

Life cycle assessment (LCA) is a typical method for the evaluation of the environmental impact of a process or plant. Particularly, greenhouse gas emission is an essential environmental indicator for an energy system [51]. Therefore, this study mainly focuses on the greenhouse gas emission of the NEHRES for environmental assessment. The daily greenhouse gas emissions, the second objective function of the optimization model, is quantified based on the LCA results. The calculation of daily GHGe is shown below:

$$GHGe = (\sum_k \sum_{t=0}^{23} q_{GHG,k} \cdot P_{k,t}) - (\sum_p \sum_{t=0}^{23} W_{co_2/c} \cdot M(C)_{p,t}) \tag{22}$$

where $q_{GHG,k}$ is the unit amount of greenhouse gas emission of component k based on LCA. $P_{k,t}$ is the amount of power produced from component k at time t. $W_{CO2/C}$ is the carbon stability factor, and $M(C)_{p,t}$ is the amount of fixed carbon generated by process p at time t.

3.3.3 Constraints

In the real world, optimization problems are usually carried out under the constraints of physical mechanisms, standards and regulations, and limits of system operation. For the design of NEHRES, there are also various constraints involved in its optimization, including the energy balance, resource limit, and system operation boundaries.

- Energy balance

The energy balance, describing the relation of energy streams flowing in and out of different components in the NEHRES, is shown in the below equation:

$$(\sum_{k} P_{gen,k,t}) - S_{in,t} + S_{out,t} \geq P_{sell,t} \tag{23}$$

where $P_{gen,k,t}$ is the amount of electricity generated by technology k at time t. $S_{in,t}$ and $S_{out,t}$ are the amount of electricity entering into and discharging from the energy storage system at time t. $P_{sell,t}$ is the amount of electricity sold to the consumers at time t. Because of the inevitable loss of electricity through its transmission, the net energy flowing out of all the system components (including the energy storage) at any time should be more than the amount of electricity sold to the grid.

- Resource limit

The available land area and the availability of solar, wind, and biomass resources set the limits of the scale of the system and the maximum amount of energy generated from the system. These constraints are formulated in the following equations:

$$\sum_{k} A_k \cdot P_{capacity,k} \leq L_{total} \tag{24}$$

$$P_{gen,k,t} \leq P_{resource,k,t} \tag{25}$$

where A_k is the unit footprint each component k. $P_{capacity,k}$ is the capacity of component k. L_{total} is the land area available for the establishment of the system. $P_{gen,k,t}$ is the amount of electricity generated from component k at time t, and $P_{resource,k,t}$ is the maximum amount of electricity generated from component k at time t caused by the limitation of solar, wind, and biomass resources.

- System operation boundaries

In addition to the energy balance and resource limit constraints, the electricity flows in the NEHRES are also constrained by the following operation boundaries of the system:

$$0 \le P_{gen,k,t}, P_{sell,t},\ S_{in,t}, S_{out,t} \tag{26}$$

$$\max_t P_{gen,k,t} \le P_{capacity,k} \tag{27}$$

$$P_{sell,t} \le D_t \tag{28}$$

$$S_{out,t} \le SOC_t \tag{29}$$

$$S_{in,t} \le P_{capacity,storage} - SOC_t \tag{30}$$

$$\Delta x \le dx\ \ (x = P_{gen,k,t}, P_{sell,t},\ S_{in,t}, S_{out,t}) \tag{31}$$

where $P_{gen,k,t}$ is the amount of electricity generated from component k at time t and $P_{sell,t}$ the amount of electricity sold to the consumers. $S_{in,t}$ and $S_{out,t}$ are the amount of electricity entering into and discharging from the energy storage system at time t, respectively. $P_{capacity,k}$ is the capacity of component k, D_t is the electricity demand at time t, and SOC_t is the state of charge of the energy storage system. Δx is the change of power between the beginning and the end of one time interval and dx is the maximum allowable rate of change of power.

3.3.4 Stochastic Optimization and the Overall Optimization Model

Typically, an optimization can be carried out using Eq.(1)-(31) deterministically (i.e., deterministic optimization) when perfect information about the model parameters are known. However, it is hard to ensure perfect knowledge of all parameters, especially of the availability of the natural resources in the future, at the time of designing the NEHRES. As uncertainty exists, optimizing the design of the NEHRES in a deterministic manner may lead to suboptimal decisions [52]. Seasonal variations of the solar, wind, and temperature profiles would consequentially lead to the stochastic states of the system operation, the life-cycle costs, and carbon dioxide emission of the NEHRES. Therefore, the uncertainty of the energy generation caused by the temporal fluctuations or seasonality of solar and wind resources should be taken into account on top of the multi-objective optimization. To take into account the uncertainties, a stochastic programming approach is incorporated in the optimization model. Specifically, the design of the NEHRES is modeled as a two-stage stochastic programming problem, where the 1st stage and 2nd stage variables stand for "here-and-now" and "wait-and-see" decisions, respectively. "Here-and-now" decisions should be made before the uncertainty is revealed, while "wait-and-see" decisions are determined afterward. Figure 3 illustrates a two-stage stochastic optimization with five uncertain scenarios. After the uncertainty is revealed, scenarios S_1 to S_5 may happen with probabilities π_1 to π_5. Although different scenarios have the same 1st stage decision, they have different 2nd stage decisions and therefore different economic and carbon sequestration performances. Since all these scenarios could happen, the stochastic optimization can be used to find out the optimal 1st stage decision variables that maximize the overall system profit and the carbon sequestration ability accounting for all the possible scenarios and their probability of realization.

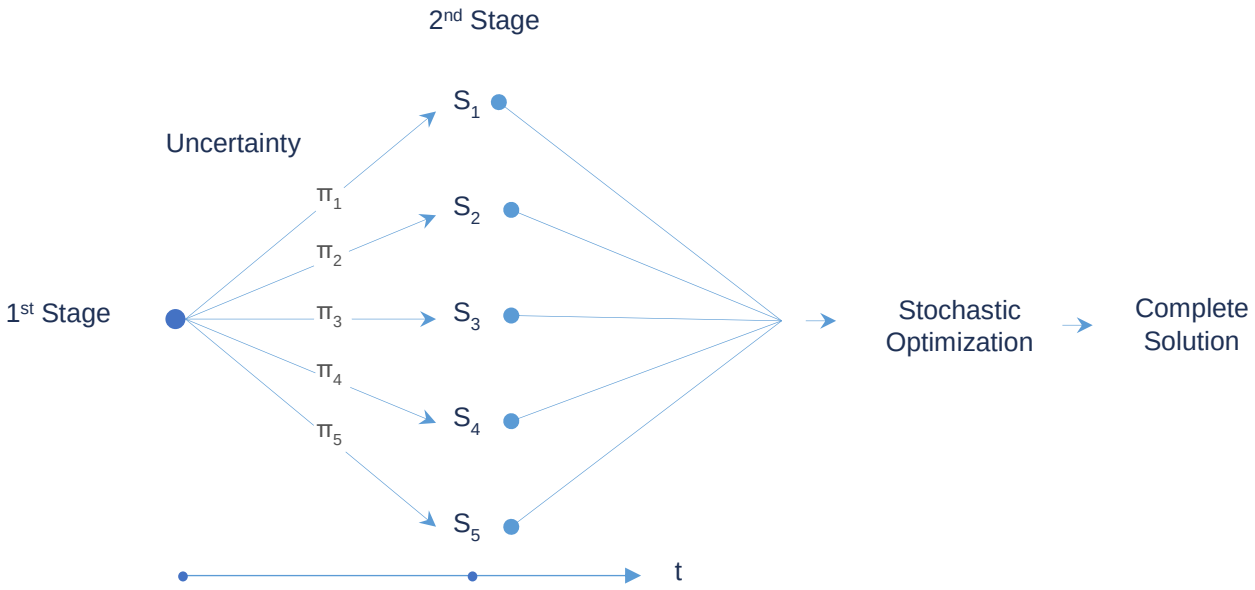

Figure 3. Illustration of a two-stage stochastic optimization.

For the design of a NEHRES, the 1st stage decision variables are the capacities of the system components. The 2nd stage decision variables are the amount of resource fed to each system component, the generation, storage and sales of electricity, and the production of biochar. Therefore, the model of the multi-objective stochastic optimization problem can be summarized below:

$$\max \quad NCF = -FC + \sum_{s=1}^{12}\{[\sum_{t=0}^{23}(Revenue_{t,s} - VC_{t,s})]\cdot \pi_s\} \tag{32}$$

$$\min \quad CO_2 = \sum_{s=1}^{12}\{[(\sum_{k}\sum_{t=0}^{23} q_{CO_2,k}\cdot P_{k,t,s}) - (\sum_{p}\sum_{t=0}^{23} w_{co_2/c}\cdot m_{c,p,t,s})]\cdot \pi_s\} \tag{33}$$

s.t.

$$(\sum_{k} P_{gen,k,t,s}) - S_{in,t,s} - S_{out,t,s} \geq D_t \tag{34}$$

$$\sum_{k} A_k \cdot P_{capacity,k} \leq L_{total} \tag{35}$$

$$P_{gen,k,t,s} \leq P_{resource,k,t,s} \tag{36}$$

$$0 \leq P_{gen,k,t,s}, P_{sell,t,s},\ S_{in,t,s}, S_{out,t,s} \tag{37}$$

$$\max_{t,s} P_{gen,k,t,s} \leq P_{capacity,k} \tag{38}$$

$$P_{sell,t,s} \leq D_{t,s} \tag{39}$$

$$S_{out,t,s} \leq SOC_{t,s} \tag{40}$$

$$S_{in,t,s} \le P_{capacity,storage} - SOC_{t,s} \tag{41}$$

$$\Delta x \le dx \ (x = P_{gen,k,t,s}, P_{sell,t,s}, \ S_{in,t,s}, S_{out,t,s}) \tag{42}$$

To obtain the Pareto optimal solutions for the multi-objective stochastic optimization problem, the nonlinear programming problem (NLP) is solved in GAMS using the Baron solver.

3.4 POST-OPTIMALITY ANALYSIS

In the absence of preference criteria provided by the decision-makers, the non-dominated solutions from multi-objective optimization, which are the points on the Pareto-curve, are not comparable since they are equally good by definition [53]. Although the decision space has substantially decreased after the optimization, it is still necessary to make the single final decision on the design of NEHRES among the set of Pareto solutions. Therefore, the post-optimality analysis should be used in the final step of the decision-making process.

For the post-optimality analysis, the technique for order of preference by similarity to ideal solution (TOPSIS) is used [54]. This method relies on the user-defined ideal (desired) and non-ideal (undesired) solutions. It takes into account the similarity of each Pareto solution to the ideal and non-ideal solutions.

The TOPSIS analysis is carried out in the following three steps:

1. Collect the preference information from the decision-maker (i.e. the user-defined ideal and non-ideal solutions, the value of which for this study will be given in the following description).
2. Calculate the evaluation matrix D_m using the following equations:

$$D_m = \frac{ED_m^{non-ideal}}{ED_m^{ideal} + ED_m^{non-ideal}} \tag{43}$$

$$ED_m^{non-ideal} = \sqrt{\sum_n (f_{m,n} - f_n^{non-ideal})^2} \tag{44}$$

$$ED_m^{ideal} = \sqrt{\sum_n (f_{m,n} - f_n^{ideal})^2} \tag{45}$$

   where $ED_m{}^{non\text{-}ideal}$ is the Euler distance between the user-defined non-ideal solution and each Pareto solution m, while $ED_m{}^{ideal}$ is the Euler distance between the user-defined ideal solution and each Pareto solution m. $f_{m,n}$ is the value of objective function n of each Pareto solution m, $f_n{}^{non\text{-}ideal}$ is the non-ideal value of objective function n specified by the decision maker, and $f_n{}^{ideal}$ is the ideal value of objective function n specified by the decision maker.
3. Obtain the "best solution" by ranking the Pareto solutions according to D_m. A Pareto solution with a larger D_m in the TOPSIS has a higher ranking.

In this study, a net-zero-emission scenario for the whole island is defined by the decision maker as an ideal solution by assuming that greenhouse gas released from the other sectors (e.g., residential, transport, industrial) on the island is totally absorbed by the NEHRES ($f_{GHGe}{}^{ideal}$ = -

3866 kg $CO_{2\text{-eq}}$/day). Moreover, the profit of a NEHRES in the ideal case is assumed to be the same as a fossil fuel based energy system (f_{NCF}^{ideal} =263 US$/day). On the contrary, the non-ideal solution has the maximal possible greenhouse gas emission released from the NEHRES by feeding all biomass into combustion ($f_{GHGe}^{non\text{-}ideal}$ = 4538 kg $CO_{2\text{-eq}}$/day) and no profit generation ($f_{NCF}^{non\text{-}ideal}$ =0 US$/day), as illustrated in Figure 4.

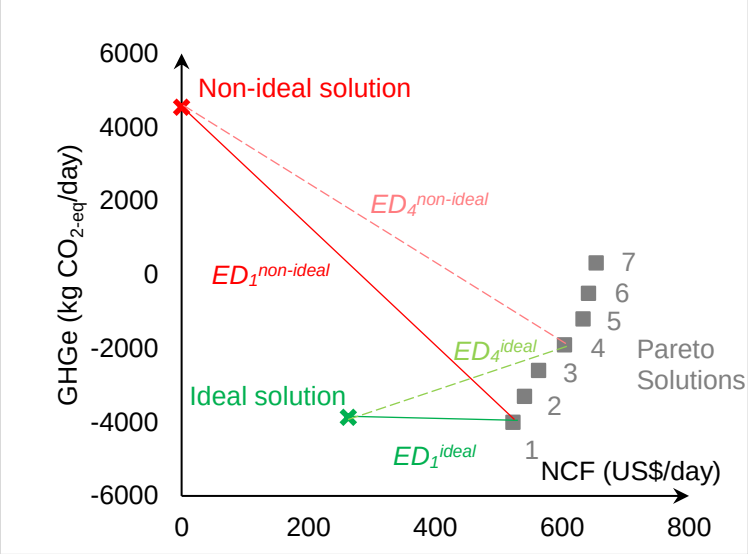

Figure 4. An example of TOPSIS analysis for the NEHRES design problem.

4 Case Study Scenario Setting

The NEHRES is suitable for an off-grid agriculture-based island, where there are abundant biomass resources in the form of agricultural residues throughout the year in addition to solar and wind resources. The application of the NEHRES concept and framework is examined using a case study based on Carabao Island (also called San Jose Island) in the Philippines.

Carabao Island is a rural island with a population of 10,881 people and an area of 22.05 km^2 [55]. Currently, the electricity supply on the island is only available from 2 pm to 6 am [56]. With the potential renewable resources on Carabao Island, it is possible to design a NEHRES to meet the local electricity demand in a green and self-sustained manner.

Information about Carabao Island is collected as an input to determine the design of the NEHRES. The solar radiation, wind speed, and temperature information on Carabao Island are shown in Figure 5. Currently, there is a lack of specific data on the availability of agricultural residues and the electricity demand on the island. Rice, sugarcane, and coconuts are the three major crops produced in the Philippines. Since Carabao Island is a rural island planned for the development of eco-farming and eco-tourism, the amount of potential crop residues on the island is forecasted based on the annual yields of the agricultural wastes in the Philippines. The biomass availability and their compositions are listed in Table 3 [57]. The local electricity demand is estimated based

on capital electricity production from the Luzon area. The estimated daily electricity profile on Carabao Island is shown in Figure 6.

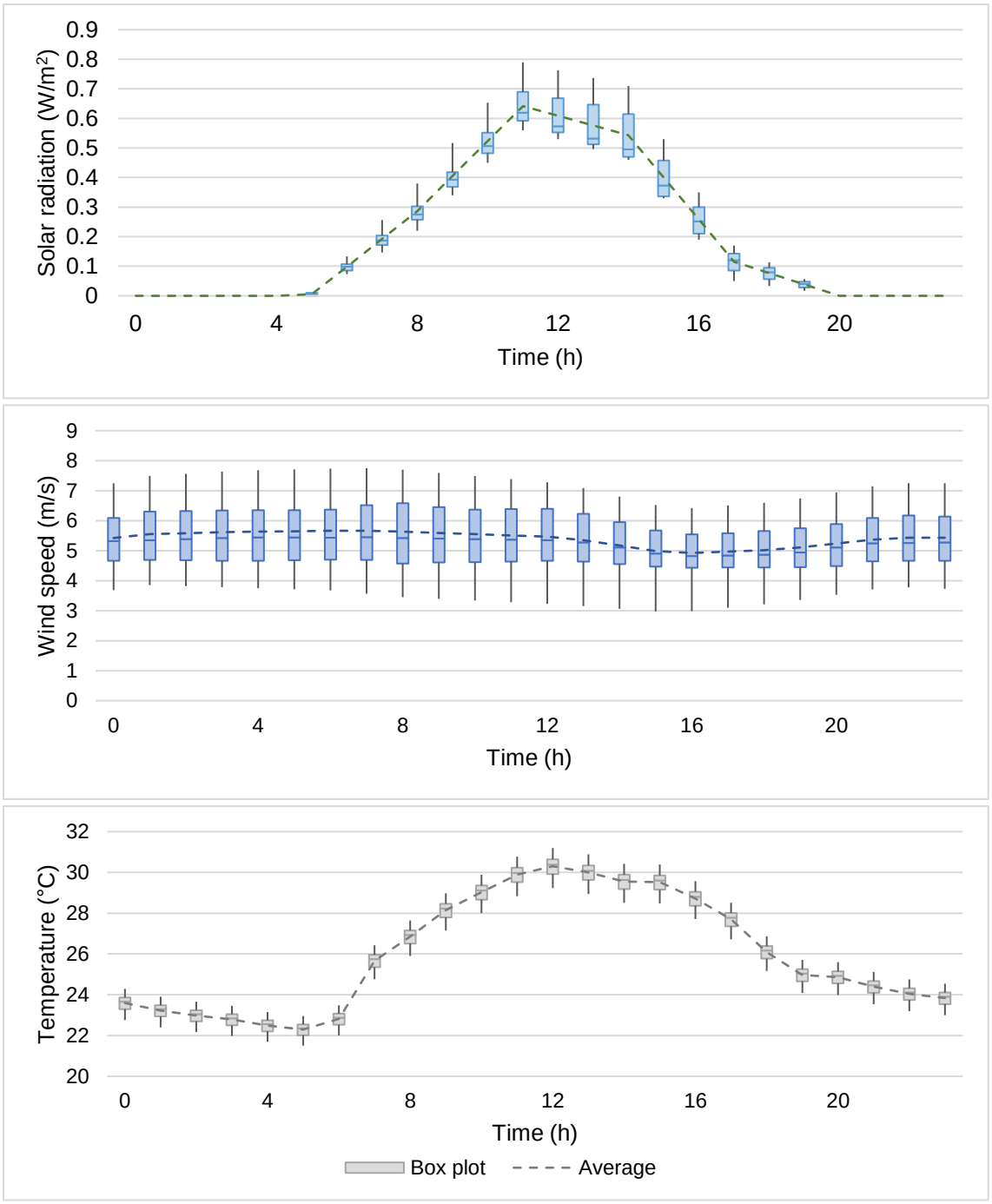

Figure 5. The box plots and average profiles of the solar radiation, wind speed, and temperature on Carabao Island for 24 hours [58].

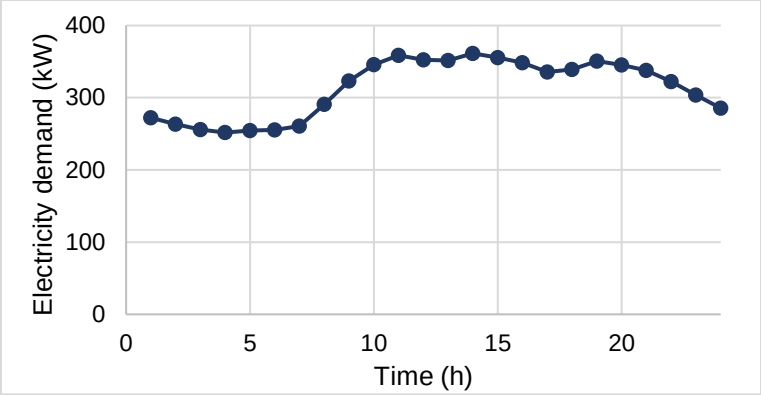

Figure 6. The estimated 24-hour electricity profile on Carabao Island [59].

Table 3. Compositions of different feedstock.

	Mass flowrate (kg/h)	C[1] (w%)	H[1] (w%)	N[1] (w%)	O[1] (w%)	Lignin[1] (w%)	MC[2] (w%)	VM[2] (w%)	FC[2] (w%)	Ash[2] (w%)	HHV (MJ/kg)
Sugarcane	51.42	41.58	5.80	0.45	52.09	21.6	9.92	81.55	06.9	11.7	17.74
Bagasse	51.42	49.86	6.02	0.16	43.89	11.21	10.39	76.72	10.71	2.44	17.16
Rice Husk	30.16	39.60	6.00	0.70	53.7	16.02	11.22	48.31	22.2	20.6	10.29
Rice Straw	41.25	49.15	6.23	1.59	42.13	36.1	11.73	57.92	12.56	20.15	13.71
Coconut shell	23.37	51.20	5.60	0.3	43.10	30.1	4.40	67.40	25.24	3.1	18.2
Coconut coir	14.95	42.1	5.5	0.2	34.6	33.5	9.4	69.6	13.2	17.2	18.89
Coconut frond	67.13	42.3	5.7	4.4	45.6	29.4	4.4	67.4	25.3	8.4	19.24

[1] Mass fractions of C, H, N, O, and lignin listed on dry ash-free (DAF) basis.

[2] Mass fractions of moisture content (MC), volatile matters (VM), fixed carbon (FC) and ash listed on a wet basis.

5 RESULTS AND DISCUSSION

The proposed multi-objective stochastic optimization framework for the NEHRES design is applied to the case study on Carabao Island. In the first place, the Pareto optimal solutions are obtained for the case study. Table 4 shows the values of the daily net cash flow and greenhouse gas emissions, as well as the capacities for the power generation and storage components in the NEHRES for each Pareto solutions.

Table 4. Optimal solutions for the case study.

No.	NCF (US$/day)	GHGe (kg $CO_{2\text{-eq}}$/day)	Solar (kW)	Wind (kW)	Combustion (kW)	Gasification (kW)	Pyrolysis (kW)	Energy storage (kW)
1	455	-2795	184	162	257	49	4	77
2	514	-2500	164	108	240	65	2	23
3	549	-1750	110	82	243	65	0	25
4	555	-600	139	67	298	0	5	34
5	580	-500	101	33	286	14	1	50
6	594	0	90	23	298	0	2	43
7	603	363	95	4	298	0	0	47

In order to further interpret the results, the Pareto curve for the multi-objective optimization will be presented in Section 5.1. To make the final decision based on the optimization and the preference of the decision maker, post-optimality analysis has been carried out, and the result is shown in Section 5.2. The design of the recommended solution selected based on the decision-making framework is presented in Section 5.3. Since the input meteorology data is represented by twelve possible scenarios, there are twelve possible operation scenarios correspondingly. One of the possible operation scenarios for the recommended solution is shown in Section 5.4. The effects of constraints and uncertainty on the optimization result are discussed in Section 5.5 and 5.6. A comparison between the recommended NEHRES and other energy systems will be shown in Section 5.7. For general applications of the NEHRES to places with drastic differences in size (or population), a discussion on the scale of application is presented in Section 5.8 as further exploitation of the case study.

In addition, interested readers can find more information about a demonstration of a weekly operation of the proposed NEHRES and a sensitivity and robustness analysis of the system in Part D and E of the Supplementary Information.

5.1 PARETO CURVE FOR THE CASE STUDY

To compare different effective solutions, the trade-off between the two objective functions is depicted by the Pareto curve shown in Figure 7. Points labeled with 1-7 in Figure 7 refer to the optimal Pareto solutions with the same number defined in Table 4.

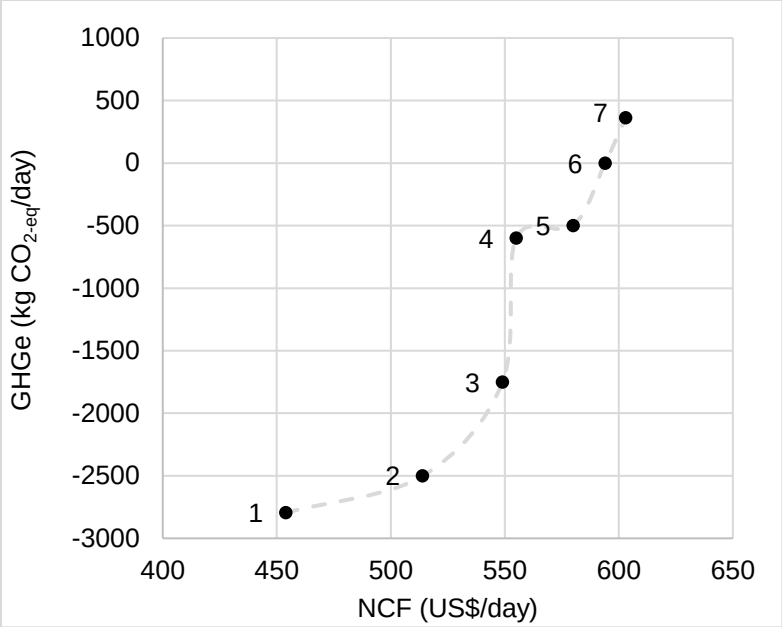

Figure 7. The Pareto curve for the multi-objective stochastic optimization of the NEHRES for Carabao Island.

From the Pareto curve, it can be found that there is no single solution of NEHRES design that can maximize the profit and minimize greenhouse gas emissions at the same time with the current set of parameters. As shown in Figure 7, the Pareto curve is monotonic, nonlinear, and nonconvex. For the optimal solutions of the NEHRES design, the net cash flow increases with increasing greenhouse gas emissions. The trend indicates that it is unable to increase the optimal net cash flow without worsening the total carbon sequestration ability of the system. Therefore, all the points on the Pareto curve are equally optimal.

Moreover, changing the system design may have a more significant effect on carbon emissions than the profitability of the NEHRES on the whole. The changing slope of the Pareto curve indicates that increasing the same amount of net cash flow at a different starting point may lead to a different level of the decline of the carbon sequestration ability of the NEHRES. Overall, by varying the design of the NEHRES the optimal NCF could change from 455 US$/day to 603 US$/day, while the GHGe would range from -2795 kg $CO_{2\text{-eq}}$ /day to 363 kg $CO_{2\text{-eq}}$/day.

5.2 Post-Optimality Analysis and Decision-Making

The results of TOPSIS analysis is shown in Figure 8, where each bar indicates the D_m value for the corresponding Pareto solution in Figure 7. A solution with a larger D_m value is preferred as it is further away from the non-ideal point and closer to the ideal point. In Figure 8, Pareto solution 1 has the largest D_m value while Pareto solution 7 has the smallest. From solution 1 to solution 7, the D_m value decreases monotonically.

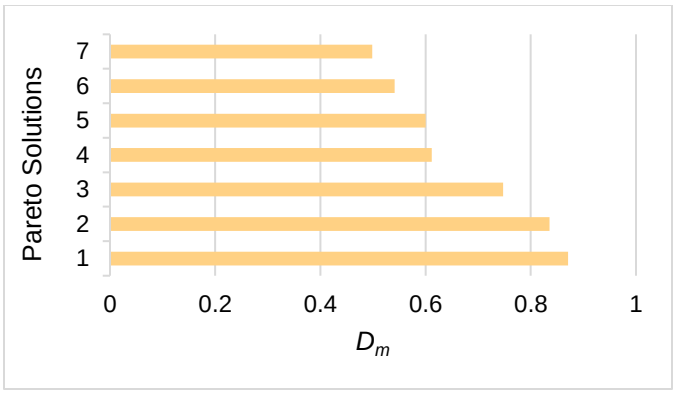

Figure 8. The result from the TOPSIS analysis of the points on the Pareto curve.

According to the quantitative assessment, the solution that minimizes the GHGe objective individually (Pareto solution 1) is the most preferred choice for the design of a NEHRES based on the current set of decision-makers' preferences. The relative position of the ideal point, non-ideal point, and the Pareto solutions of this case study can be represented in Figure 4. The recommended solution (Pareto solution 1) is the closest point to the user-defined ideal solution (263, -3866) and furthest from the user-defined non-ideal solution (0, 4538) among all Pareto solutions.

Therefore, the recommended solution for the design of NEHRES has a daily net cash flow of 455 US$/day and a greenhouse gas emissions of -2795 kg $CO_{2\text{-eq}}$/day. It is both economically and environmentally attractive compared with the user-defined ideal solution. The recommended NEHRES outperforms the user-defined ideal solution by 73% in terms of daily profit. Although the carbon sequestration performance of the recommended NEHRES is not enough to achieve the ideal scenario of net-zero emission on the whole island defined by the decision maker, it is still attractive enough to offset 72% of the total greenhouse gas released from the other sectors (residential, transport, and industrial) on the island. To provide further insight into the recommended system, the design and the operation of the components in the NEHRES are discussed in the next two sections.

5.3 DESIGN OF THE SYSTEM COMPONENTS

Figure 9 shows the capacities of the components in the recommended NEHRES.

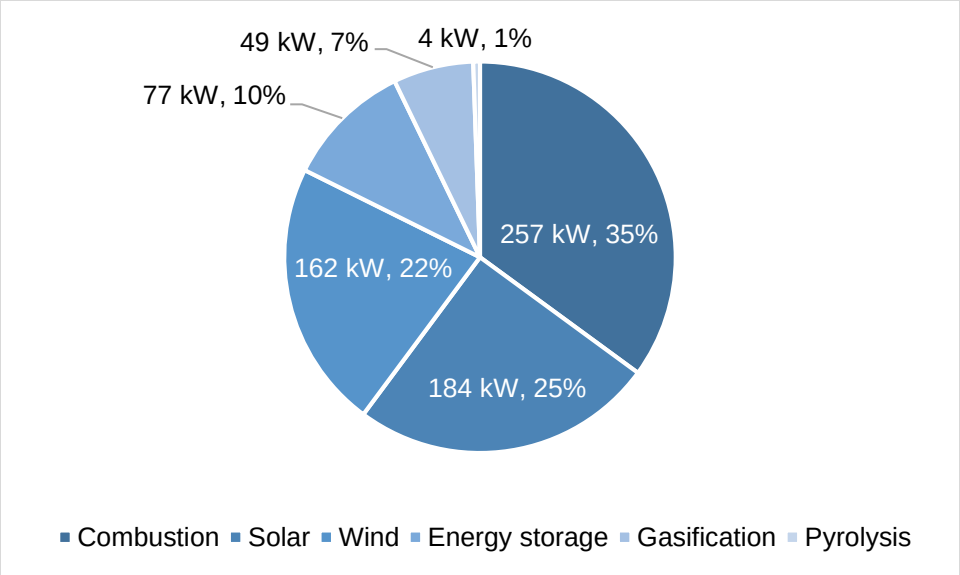

Figure 9. Capacities of the components in the recommended NEHRES.

All the candidate components are contained in the recommended NEHRES. Combustion has the largest capacity (257 kW) among all the major components in the recommended NEHRES, accounting for 35% of the capacity of the whole NEHRES. The joint capacity of solar and wind power generation takes up nearly half of the total system capacity. The solar PV system is 162 kW, containing 1038 PV panels with panel size 1.5m×0.8m. The 184 kW wind power generation system includes 47 wind turbines, each of which has a rotor diameter of 7.2 m. The energy storage system is a vanadium redox battery (VRB) with a capacity of 77 kW. Last but not least, the gasification and pyrolysis systems have power capacities of 49 kW and 4 kW, respectively. Although these two processes generate less electricity than the other components, they produce all the biochar for the NEHRES. As the design of the NEHRES is tightly related to the system operation, the information on the operation of the NEHRES is needed to fully understand the result for the NEHRES design.

5.4 Operation of the system components

After the realization of the uncertain meteorology scenarios, twelve optimal operation scenarios are generated. For the operation of the NEHRES, the amount of generation, storage, and sales of products are of major concern. One possible operation scenario of the recommended NEHRES is demonstrated here. Figure 10 shows the one possible scenario of the generation, storage, discharge and sales of electricity of the recommended NEHRES. Figure 11 shows the one possible scenario of the biochar generation from the NEHRES, which is further broken down into the amount of biochar derived from gasification and pyrolysis processes.

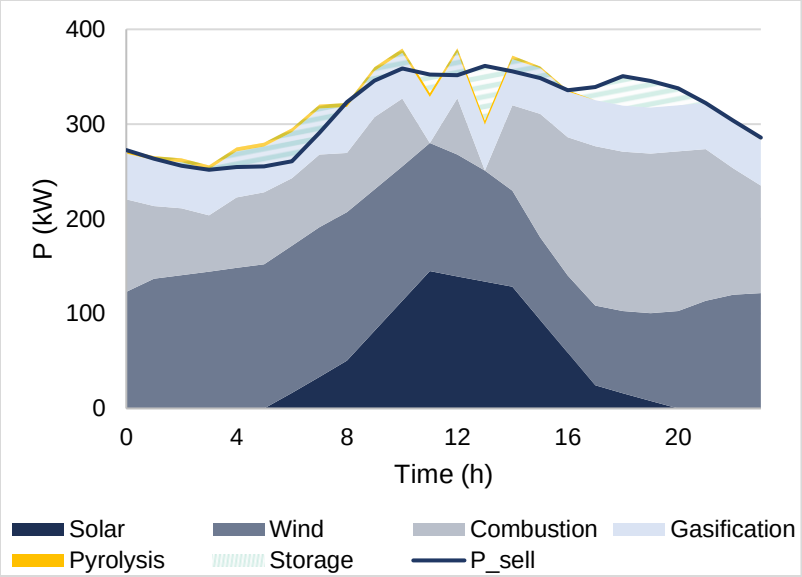

Figure 10. One possible scenario of the 24-hour electricity profile of the recommended NEHRES.

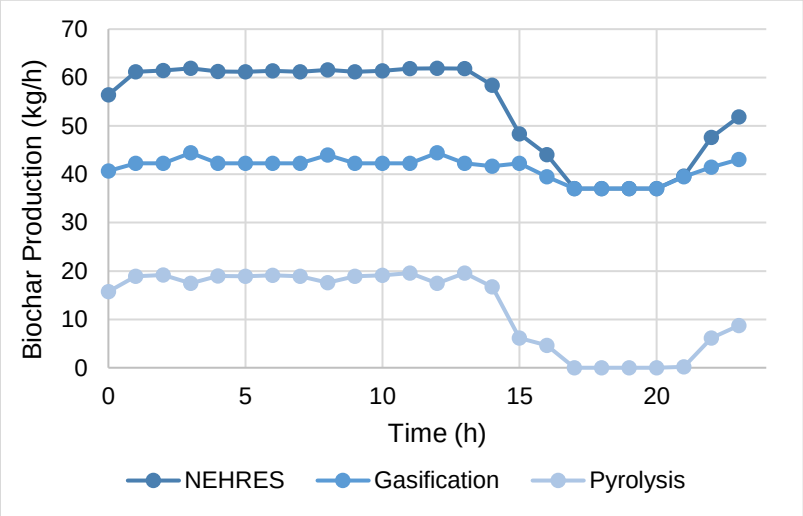

Figure 11. One possible scenario of the 24-hour biochar production profile of the recommended NEHRES.

Figure 10 is a stacked area plot that depicts the electricity flows in the NEHRES. The solar power generation starts at 6:00, peaks at 11:00, and decreases to zero at 20:00. Since there is no solar radiation before 6:00 or after 20:00, there is no electricity generation during these time intervals. Unlike solar power generation, electricity is generated from the wind and gasification continuously throughout the day. Combustion also generates a large amount of electricity in the day although there are two one-hour breaks for the combustion components seen at 11:00 and 13:00. Pyrolysis is under operation for 20 hours except for the period from 17:00 to 21:00. The energy storage component is working for an electric charge from 1:00 to 11:00, during 12:00, and from 14:00 to

16:00. The stored electricity is discharged from the energy storage component during 11:00, 13:00, and from 17:00 to 21:00. In this scenario, all the components installed in the NEHRES take part in the electricity generation or storage.

With respect to biochar production, the amount of biochar derived from gasification is about 40 kg/h throughout the day as shown in Figure 11. In the pyrolysis process, the biochar production rate is about 18 kg/h before 14:00, decreases to about 6 kg/h for 2 hours, turns to zero production for the following 4 hours, and gradually increases to 8.7 kg/h during the remaining 3 hours.

The wind component generates the largest amount of electricity throughout the day, followed by combustion, gasification, solar, and pyrolysis. Since the recommended solution is the case where the GHGe emission is the minimum among all the possible designs of the NEHRES, pyrolysis is a preferable technology due to its highest carbon sequestration potential among all candidates. Gasification is the second top-ranking technology for carbon sequestration. For the remaining three technologies, combustion has a larger life-cycle greenhouse gas emission than wind energy systems whereas the solar PV system has an even higher emission value than combustion throughout its life cycle. Therefore, pyrolysis and gasification should be the most favorable choices for both the design and operation of the NEHRES. If there is no system or resource limitation, pyrolysis would be the only component in the system when the GHGe objective is minimized because it can produce the largest amount of biochar while generating electricity. However, for the recommended NEHRES, not all the generation duty is allocated to pyrolysis. This contradiction to the ideal design and operation is caused by the resource limit, which will be illustrated in the next section.

5.5 Effect of Supply-Demand Constraints

The optimal design and operation of the NEHRES are not only affected by the objectives in the optimization, but also the constraints. Moreover, the design and operation of the NEHRES are interactive in the optimization. The possible operation of the NEHRES is constrained by the resource limit and the design capacity of the components in the system. In this section, the effect of the constraints on the design and operation of the recommended NEHRES is discussed.

To demonstrate the effects of the resource limit constraint, three extreme scenarios are created based on two assumptions. Firstly, it is assumed that the solar and wind components of the recommended NEHRES are optimally operated to utilize the maximum available solar and wind resources, which is also the same as the operation scenario for the recommended NEHRES discussed in Section 5.4. Secondly, the capacities of the combustion, gasification, and pyrolysis components are set to be unbounded and all the biomass feedstock are fed into one of the three components for each extreme scenario. Figure 12 shows the three extreme scenarios when fully utilizing solar, wind, and biomass resources via different biomass conversion processes.

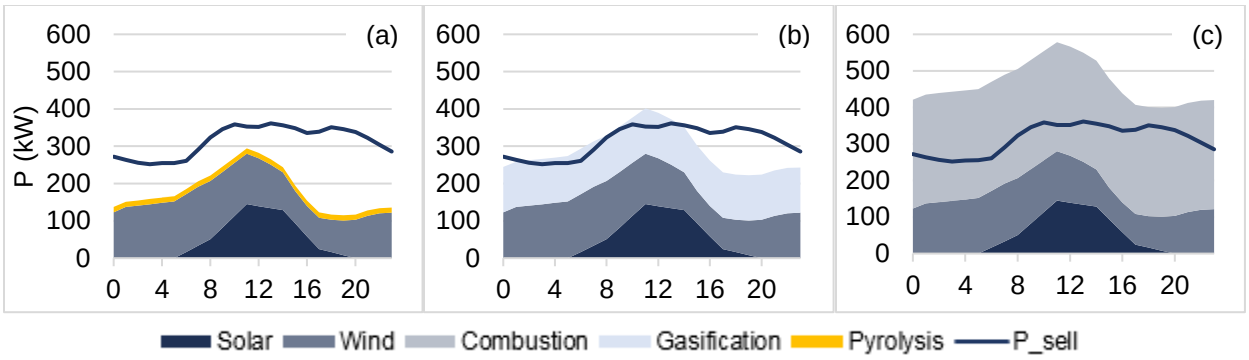

Figure 12. The electricity generation profiles with full utilization of the solar, wind, and biomass resources: (a) solar-wind-pyrolysis; (b) solar-wind-gasification; (c) solar-wind-combustion.

In this study, meeting the electricity demand is a constraint for the NEHRES design. From Figure 12, it can be found that feeding all the biomass feedstock to pyrolysis (shown in Figure 12(a)) or gasification (shown in Figure 12(b)) is unable to meet the electricity demand. The three biomass conversion technologies are competing for limited biomass resource. For the recommended NEHRES where the greenhouse gas emission is preferred to be minimized, pyrolysis has the priority to utilize the biomass feedstock due to its highest carbon sequestration potential among the three processes, followed by gasification, and lastly the combustion process. Because case (a) in Figure 12 cannot fulfill the electricity demand, a proportion of biomass would be redistributed to the gasification process and then the combustion process to satisfy the constraint. Therefore, the resource limit constraint determines the necessity of gasification and combustion component in the recommended NEHRES even though they have larger net greenhouse gas emission than pyrolysis, which explains the contradiction mentioned at the end of the last section (Section 5.4).

In addition, due to the uncertain weather conditions, solar and wind resources can be far less than the current scenario. In order to satisfy the electricity constraint, the optimal design of NEHRES obtained by stochastic optimization should be able to deal with the worst-case scenario where there are little wind and solar resources. As a result, the capacity of the combustion component obtained from stochastic optimization would be higher than that obtained from the deterministic optimization under this specific weather scenario, which explains why the combustion component has the largest design capacity among all the components in the recommended NEHRES.

5.6 Effect of Uncertainty

To further understand the effects of uncertainty on the design of NEHRES, the same optimization procedure is carried out using a deterministic model, in which the mean value of each meteorology parameter is used to replace the set of different weather scenarios of the stochastic model. The key results of the deterministic optimization are shown in Figure 15.

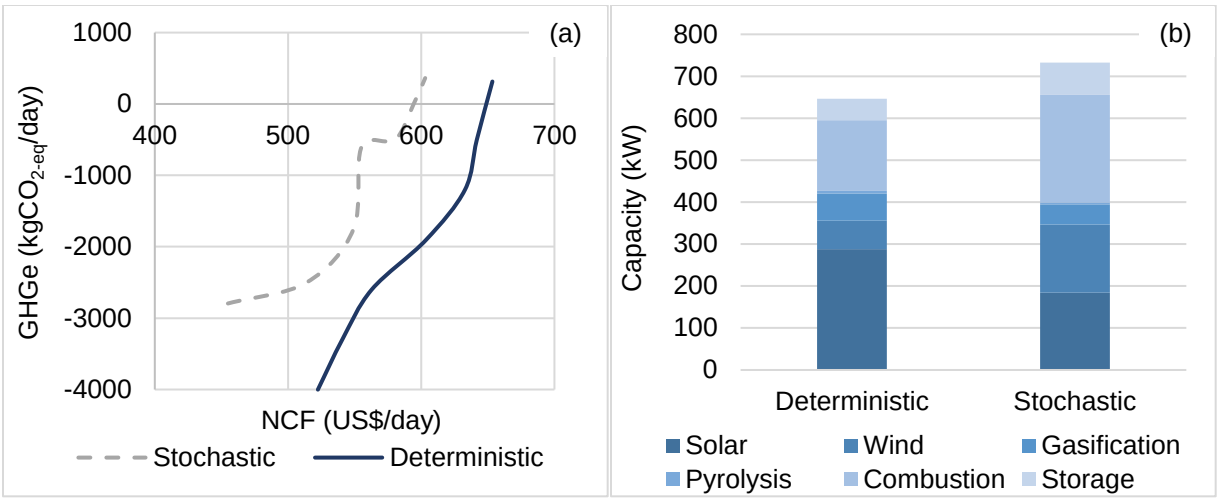

Figure 13. Results for the deterministic optimization of the NEHRES: (a) Pareto curve; (b) Capacities of different components in the NEHRES.

Figure 13 demonstrates that the consideration of uncertainty of weather conditions will lead to a more conservative design which has a larger combustion capacity and a larger capacity of the whole system to ensure secure electricity supply under all possible uncertain scenarios. This would also lead to less profit or more GHGe compared with the model that ignores uncertainties. Figure 13 (a) shows the Pareto curve of the deterministic model is to the right of the stochastic model, indicating a higher profit resulted from the deterministic model than the stochastic model under a fixed GHGe value. Figure 13 (b) shows the total capacity of the NEHERS system obtained from a stochastic optimization is larger than that of a deterministic optimization. The solution obtained from the stochastic model has larger combustion, wind, and storage capacities and smaller solar, gasification, and pyrolysis capacities. As it is mentioned in Section 5.5, the larger capacity of the combustion component derived from a stochastic model attributes to the consideration of the worst-than-average weather conditions for electricity generation. Because wind and energy components are non-biomass-based technologies with smaller GHGe compared with combustion, the capacities of wind and energy storage components of the NEHRES also increase to mitigate greenhouse gas emission with expanded combustion capacity in a stochastic model.

5.7 COMPARISON WITH OTHER ENERGY SYSTEMS

In order to compare the performance of NEHRES with other energy systems, the levelized GHGe and the leverlized profit for different energy storage systems are calculated. The Asia-specific levelized cost and the GHGe data of a range of representative energy systems is a from the literature. The values for NEHRES is based on the proposed optimization results while the local electricity price together and the levelized cost data are used to estimate the levelized profit for other energy systems. Figure 14 and 15 show the levelized GHGe and levelized profit of the proposed NEHRES and the other energy systems.

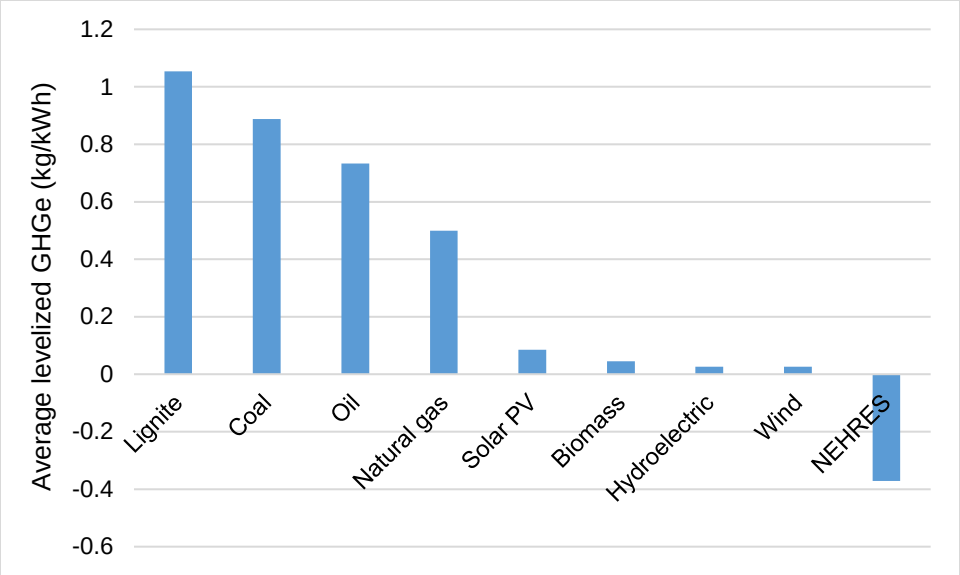

Figure 14. The levelized GHGe of the proposed NEHRES and the other energy systems.

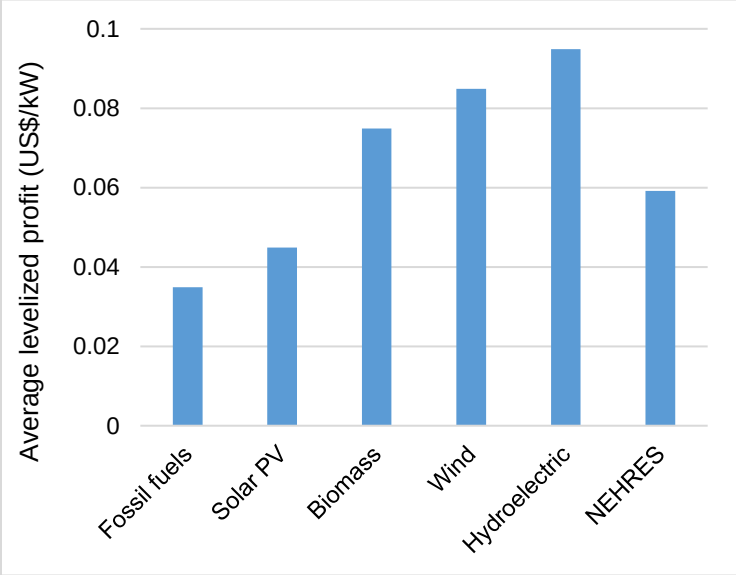

Figure 15. The levelized profit of the proposed NEHRES and the other energy systems.

Compared with other energy systems, the recommended NEHRES has greenhouse gas reduction (negative emission) potential while others do not. As shown in Figure 14, the recommended NEHRES has the potential to sequestrate 0.37 kg $CO_{2\text{-eq}}$ greenhouse gas for each kW of electricity generation. In contrast, other energy systems release greenhouse gas during electricity generation. Particularly, fossil fuels (lignite, coal, oil, and natural gas) release the largest amount of greenhouse gas (at least 0.5 kg $CO_{2\text{-eq}}$ /kW) among the energy systems. As an example of comparison, the recommended NEHRES is able to offset approximately half of the GHG released by a coal fire power system while producing the same amount of electricity.

In terms of economic performance, the recommended NEHRES has a competitive economic performance compared with other energy systems. As shown in Figure 15, the recommended NEHRES has a levelized profit lying between a single solar PV system and a single biomass power generation system. It is less profitable than the biomass, onshore wind, and hydroelectric power generation systems, however, it is more economical than a fossil-fuel based energy system in the long run due to the low cost of energy sources.

Despite the economic feasibility and the environmental benefits of the NEHRES, the technical feasibility is a critical issue for its deployment. The proposed NEHRES is a hybrid system of solar, wind, combustion, gasification, and pyrolysis technologies. At the current stage, solar and wind are relatively mature technologies with a large scale of commercialization. Most of the energy storage technologies also have a high technology readiness level. However, the bottleneck lies in the gasification and pyrolysis technologies as they are still under the technology development and demonstration phase. To facilitate the realization of the NEHRES, more effort is needed for the development and commercialization of the gasification and pyrolysis technologies.

5.8 APPLICATION OF THE NEHRES TO DIFFERENT SCALES

Scalability is also a critical feature for the application of NEHRES. To validate the generalization of the NEHRES to places with drastic variations in size (or population), the Carabao case study is used as the base case, and several new scenarios are generated for an investigation of scale-up effect. The electricity demand and the maximum available solar, wind, and biomass resources of the new scenarios are assumed to be 2-6 times of those in the based case while other parameters remain the same. The same optimization procedure is conducted for the new scenarios. The result of the Pareto curves for the application of the NEHRES to different scales is shown in Figure 16.

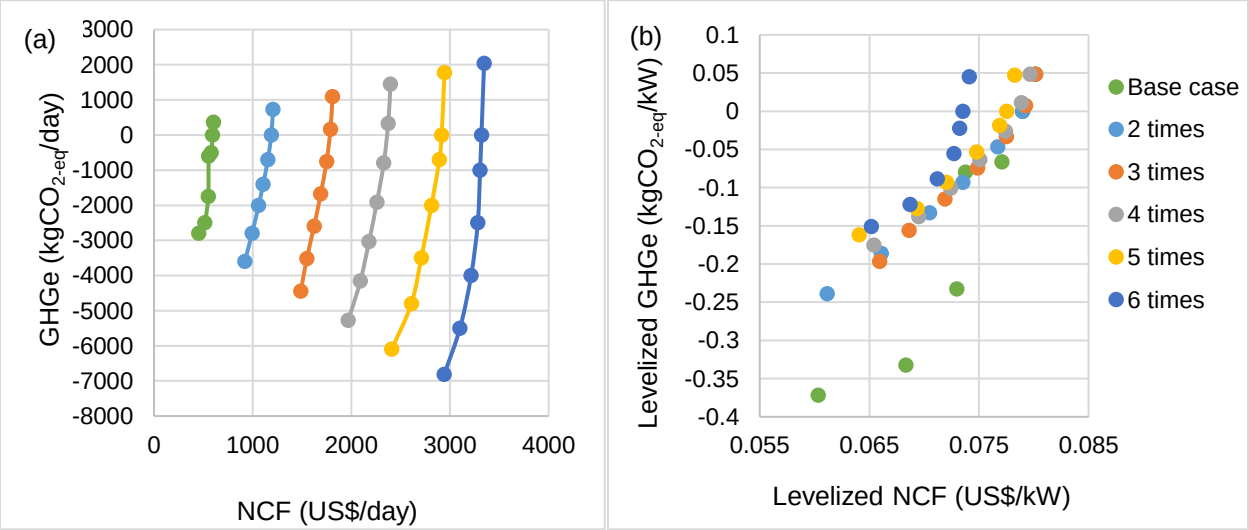

Figure 16. Pareto curves for different scales of applications of the NEHRES.

Changing the scale of application of the NEHRES has an apparent effect on the daily NCF and daily GHGe. According to the optimization result, increasing the scale of application would

generally lead to a larger NEHRES, a larger daily profit, and a larger range of daily GHGe. In Figure 16 (a), the Pareto curve shifts to the right for a larger scale of application. In other words, the system could earn more daily profit under the same GHGe level (or sequestrate more carbon with the same daily NCF) for a larger scale of application.

However, a different trend is observed when interpreting the two objective values in the unit of profit or GHGe per kW of electricity (i.e. levelized value). Figure 16 (b) shows the levelized NCF and levelized GHGe under different scales of applications. At first glance, it can be found that the levelized values are less sensitive to the scale of application compared with Figure 16 (a). Moreover, the small-scale NEHRES are generally more efficient than the larger ones in terms of levelized NCF and levelized GHGe. Therefore, the optimal NEHRES of a small-scale application can be designed as a basic module, and the optimal design of the NEHRES for a larger scale application under the same weather, market, and economic conditions can be achieved by simply multiplying the small-scale basic module.

Practically, the basic NEHRES module can be designed in a community level which could be implemented with the microservices framework. In this concept, scaling up can be carried out by multiplying the module in the large-scale region to multi-communities level. For example, we can assume a standard community is based on 2000 households for a population of 10,000-15,000 people, which is approximately equivalent to the base case of this study (Carabao case study). To design the NEHRES for a large-scale application such as a region with a population of one million, a community-level NEHRES can be first designed for the standard community using the proposed decision-support framework. Then the large-scale region can be split into 100 communities, each of which powered by the optimal community-level NEHRES module. With the generalization of optimal community-level NEHRES, we could cut down the investment of large power plants, get rid of the dependency of fossil fuels and loss of electrification due to long-distance transmission of electricity, and meanwhile cut down the investment of step-up power station to counter the long-distance electrification loss. From this, we could maintain maximum carbon sequestration with biochar application to soil, as well as a maximum the energy utilization and cost efficiency with a harvest of hybrid renewable energy.

6 CONCLUSIONS AND FUTURE WORK

In this paper, the concept, system modeling, and optimal design and assessment of a negative emission hybrid renewable energy system (NEHRES, a hybrid PV-wind-biomass renewable energy system with biochar production) have been presented. A multi-objective stochastic decision-support framework has been developed to maximize the daily net cash flow and minimize the greenhouse gas emissions of the whole system. Through a case study on a stand-alone rural island, we investigated the trade-off between carbon sequestration and economic benefit for a NEHRES, demonstrated the system design and operation and sensitivity and robustness of the system subject to different scenarios, compared the performance of proposed system with general

energy generation benchmarks, and discussed the potential application of the system to different scales. The major findings of the study are summarized as follows:

- The results show that for the island with a population of 10,881 people and an area of 22.05 km^2, a 162 kW solar power component (1038 PV panels), a 184 kW wind power component (47 wind turbines), a 257 kW combustion component, a 49 kW gasification component, a 4 kW pyrolysis component, and a 77 kW vanadium redox battery energy storage component constituted the optimal configuration of the negative emission hybrid renewable energy system.
- The proposed solution has a daily net cash flow of 455 US$/day and a greenhouse gas emissions of -2795 kg $CO_{2\text{-eq}}$/day. It is both economically and environmentally attractive compared with other energy systems and the user-defined ideal solution. Although a net-zero emission of the whole island under study is challenging to achieve with the proposed system, it is still potential to offset 72% of the total greenhouse gas released from the other sectors (residential, transport, and industrial) on the island.
- The sensitivity study about the effect of scale on the optimal design of NEHRES shows that a small-scale system can be more efficient than the larger ones in terms of levelized net cash flow and levelized greenhouse gas emissions. Therefore, when it comes to scaling up the system, a small-scale application can be designed as a basic module to be "numbered up" for a larger scale application under the same weather, market, and economic conditions.

For future research, data-driven prediction of future renewable energy resource and demand profile can be incorporated into the data analysis step of the proposed framework to enhance and precision and the practical significance of the design. More detailed modeling of the systems, such as developing first-principle biomass conversion models, can be adopted to make the whole system more understandable and trustworthy. Surrogate optimization can also be employed to avoid a drastic increase in computational time caused by the use of more precise and complex first-principle models. Apart from the economic and environmental objectives considered in this study, further studies incorporating other factors, such as social and ecological effects, can also be carried out by adding additional constraints and objectives to the model. To be more comprehensive, expending the possible energy mix to include geothermal and ocean energy is also feasible based on the current optimization framework.

ACKNOWLEDGEMENT

This research is supported by the National Research Foundation, Prime Minister's Office, Singapore under its Campus for Research Excellence and Technological Enterprise (CREATE) programme.

NOMENCLATURE

Acronyms

AR	Afforestation and reforestation
BECCS	Bioenergy production with carbon capture and storage
$CO_{2\text{-eq}}$	Equivalent carbon dioxide emissions
DAC	Direct air capture
DAF	Dry ash free
EW	Enhanced weathering
GHGe	Greenhouse gas emission
GHGe	Greenhouse gas emission
HHV	Higher heating value
HRES	Hybrid renewable energy system
IC	Internal combustion
LCC	Life-cycle cost
NCF	Net cash flow
NEHRES	Hybrid renewable energy systems
NETs	Negative emission technologies
OF	Ocean fertilization
PV	Photovoltaic
SCS	Soil carbon sequestration
SRC	Standard rating conditions

Symbols

A	Unit footprint component k (m^2/kW)
Ar	Area swept by the rotor blades of the wind turbine (m^2)
$C_{biochar}$	Unit selling price of biochar (US$/kg)
C_{elec}	Unit selling price of electricity (US$/kW)
C_{fuel}	Unit cost of fuels (US$/kg)
C_{CAPEX}	Unit capital investment cost of the components (US$/kW)

C_p	Wind power coefficient
$C_{storage\_CAPEX\_P}$	Unit power capital investment cost of the energy storage component (US$/kW)
$C_{storage\_CAPEX\_E}$	Unit energy capital investment cost of the energy storage component (US$/kWh)
S_{max}	Power capacity of the energy storage component (kW)
SOC_{max}	Energy capacity of the energy storage component (kWh)
CRF	Capital recovery factor
$C_{storage}$	Unit cost of the operation and maintenance of the energy storage component (US$/kWh)
C_{vom}	Unit cost of the operation and maintenance of the power generation components (US$/kWh)
D_m	Evaluation matrix of the TOPSIS analysis
D_t	Electricity demand at time t (kW)
ED_i^{ideal}	Euler distance between the ideal point and each Pareto solution
$ED_i^{non\text{-}ideal}$	Euler distance between the non-ideal point and each Pareto solution i
eff_c	Electrical efficiency of an incineration plant
$eff_{thermal}$	Thermal efficiency of IC engine
eff_{WtoE}	Efficiency of converting mechanical work to electricity
F	Mass flowrate of the biomass (kg/h)
FC	Daily fixed cost (US$/day)
$f_{m,n}$	Value of objective function n of each Pareto solution m
f_n^{ideal}	Value of objective function n specified by the decision maker
$f_n^{non\text{-}ideal}$	Non-ideal value of objective function n specified by the decision maker
FOM	Fixed operating and maintenance cost (US$/h)
$Fuel$	Fuel cost of the system (US$/h)
GHGe	Greenhouse gas emissions (kg $CO_{2\text{-}eq}$/day)
HHV	Higher heating value (kJ/kg)
I	Output current of the solar panel (A)
I_d	Diode saturation current (A)

I_l	Light current (A)
$CAPEX$	Capital investment cost of the NEHRES (US$)
k	Boltzmann's constant ($1.381\times^{-23}$ J/K)
L_{total}	Land area available for the establishment of the system (m^2)
$M(C)_{gasification}$	Amount of fixed carbon derived from the gasification process (kg/h)
$M(C)_{pyrolysis}$	Amount of fixed carbon derived from the pyrolysis process (kg/h)
$m_{biochar}$	Mass production rate of biochar (kg/h)
M_C	Molecular weights of C (g/mol)
M_{CH4}	Molecular weights of CH_4 (g/mol)
M_{CO}	Molecular weights of CO (g/mol)
M_{CO2}	Molecular weights of CO_2 (g/mol)
NCF	Net cash flow ($/day)
n_I	Diode ideality factor
N_s	Number of solar PV modules
P	Power (kW)
$P_{capacity,k}$	Capacity of component k (kW)
$P_{gen,k,t}$	Amount of electricity generated by technology k at time t (kW)
$P_{k,t}$	Amount of power produced from component k at time t (kW)
P_r	Rated power of the wind turbine (kW)
$P_{resource,k,t}$	Maximum amount of electricity generated from component k at time t caused by the limitation of solar, wind, and biomass resources (kW)
P_s	Power generated by the solar panel (kW)
$P_{sell,t}$	Amount of electricity sold at time t (kW)
P_w	Power generated by the wind turbine (kW)
q	Elementary charge ($1.602\times^{-}19$ C)
$q_{GHG,k}$	Amount of greenhouse gas emission of component k (kg eq CO_2/kW)
r	Interest rate
$Revenue_t$	Hourly revenue from the sales of the products ($/h)
R_{se}	Series resistance (Ω)

R_{sh}	Shunt resistance (Ω)
$S_{1,2,3...}$	Scenarios in stochastic programming
S_{in}	Amount of energy entering the energy storage system (kW)
SOC_t	State of charge of the energy storage system (kWh)
S_{out}	Amount of energy flowing out of the energy storage system (kW)
T	Lifespan of the NEHRES (y)
$t_{1/2}$	Half-life of biochar in soil (y)
T_c	Cell temperature of the solar PV module (K)
TH	Time horizon for the evaluation of the carbon stability factor (y)
t_{op}	Number of days under operation in a year
T_p	Pyrolysis temperature (K)
U	Voltage of the PV cell (V)
v	Wind speed (m/s)
v_{ci}	Cut-in wind speed of the wind turbine (m/s)
v_{co}	Cut-out wind speed of the wind turbine (m/s)
VC_t	Variable costs (US$/h)
VOM_t	Variable operating and maintenance cost (US$/h)
v_r	Rated wind speed of the wind turbine (m/s)
$W_{CO2/C}$	Carbon stability factor
Y	Mass fraction
$Y_{C(char)}$	Mass fraction of fixed carbon contained in biochar
Y_{CH4}	Mass fraction of CH_4 in the producer gas
Y_{char}	Yield of biochar (%w of feed)
Y_{CO}	Mass fraction of CO in the producer gas
Y_{CO2}	Mass fraction of CO_2 in the producer gas
Y_{gas}	Yield of producer gas (%w of feed)
α	Ratio of fixed operating and maintenance cost to capital cost
Δt	Time interval

Δx	Change of power between the beginning and the end of one time interval
ε	Modified ideality factor
η	Round-trip efficiency
π	Probability
ρ	Air density (kg/m^3)
ρ_{gas}	Density of producer gas (kg/m^3)

Subscripts

i	Set of biomass feedstock (i=sugarcane waste, sugarcane bagasse, rice husk, rice straw, coconut shell, coconut coir, coconut frond)
j	Set of chemical composition in biomass (j=C, H, O, N, Lignin, MC, VM, FC, Ash)
k	Set of system components (k= solar, wind, combustion, gasification, pyrolysis, energy storage)
p	Set of biomass conversion process (p=combustion, gasification, pyrolysis)
t	Set of time intervals (t=0,2,3…23)

REFERENCES

[1] United Nations. Paris agreement. FCCC/CP/2015/L. 9/Rev. 1, United Nations Bonn; 2015.

[2] EASAC. Science Advice for the Benefit of Europe Negative emission technologies: What role in meeting Paris Agreement targets? 2018.

[3] IPCC. Summary for policy makers. 2014.

[4] IEA Statistics. Renewable electricity output 2018. https://data.worldbank.org/indicator/EG.ELC.RNEW.ZS?view=chart (accessed November 25, 2018).

[5] Climate Watch. Global Historical Emissions 2018. https://www.climatewatchdata.org/ghg-emissions?breakBy=sector&source=31&version=1 (accessed November 25, 2018).

[6] BP. BP Statistical Review of World Energy 2018. https://www.bp.com/content/dam/bp/en/corporate/pdf/energy-economics/statistical-review/bp-stats-review-2018-full-report.pdf (accessed November 25, 2018).

[7] IPCC. IPCC Fifth Assessment Report Lima Climate Action High Level Session Lima, Perú. 2011.

[8] IEA. Global Energy & CO2 Status Report 2017. https://www.iea.org/geco/emissions/ (accessed November 25, 2018).

[9] IPCC. Climate Change 2014: Mitigation of Climate Change. 2014.

doi:10.1017/CBO9781107415416.

[10] Yan J. Negative-emissions hydrogen energy. Nat Clim Chang 2018;8:560–1. doi:10.1038/s41558-018-0215-9.

[11] McGlashan N, Workman MHW, Caldecott B, Shah N. Negative Emissions Technologies 2012. https://www.imperial.ac.uk/media/imperial-college/grantham-institute/public/publications/briefing-papers/Negative-Emissions-Technologies---Grantham-BP-8.pdf (accessed July 29, 2018).

[12] UN Environment. Emissions Gap Report | UN Environment 2017. https://www.unenvironment.org/resources/emissions-gap-report (accessed July 29, 2018).

[13] Burns W. Carbon Removal/ Negative Emissions Technologies Bibliography 2018. https://www.american.edu/sis/centers/carbon-removal/upload/carbon_removal_bibliography_4-1.pdf (accessed November 24, 2018).

[14] McLaren D. A comparative global assessment of potential negative emissions technologies. Process Saf Environ Prot 2012;90:489–500. doi:10.1016/J.PSEP.2012.10.005.

[15] Smith P. Soil carbon sequestration and biochar as negative emission technologies. Glob Chang Biol 2016;22:1315–24. doi:10.1111/gcb.13178.

[16] Strefler J, Amann T, Bauer N, Kriegler E, Hartmann J. Potential and costs of carbon dioxide removal by enhanced weathering of rocks. Environ Res Lett 2018;13:034010. doi:10.1088/1748-9326/aaa9c4.

[17] Williamson P, Wallace DWR, Law CS, Boyd PW, Collos Y, Croot P, et al. Ocean fertilization for geoengineering: A review of effectiveness, environmental impacts and emerging governance. Process Saf Environ Prot 2012;90:475–88. doi:10.1016/J.PSEP.2012.10.007.

[18] Call for Papers: Special Issue on Negative Emission Technologies 2018. https://www.journals.elsevier.com/applied-energy/call-for-papers/call-for-papers-special-issue-on-negative-emission-technolog (accessed November 24, 2018).

[19] Schmidt MWI, Torn MS, Abiven S, Dittmar T, Guggenberger G, Janssens IA, et al. Persistence of soil organic matter as an ecosystem property. Nature 2011;478:49–56. doi:10.1038/nature10386.

[20] Lu L, Huggins T, Jin S, Zuo Y, Ren ZJ. Microbial metabolism and community structure in response to bioelectrochemically enhanced remediation of petroleum hydrocarbon-contaminated soil. Environ Sci Technol 2014;48:4021–9. doi:10.1021/es4057906.

[21] Masiello CA, Chen Y, Gao X, Liu S, Cheng HY, Bennett MR, et al. Biochar and microbial signaling: Production conditions determine effects on microbial communication. Environ Sci Technol 2013;47:11496–503. doi:10.1021/es401458s.

[22] Wu H, Lai C, Zeng G, Liang J, Chen J, Xu J, et al. The interactions of composting and biochar and their implications for soil amendment and pollution remediation: a review. Crit Rev Biotechnol 2017;37:754–64. doi:10.1080/07388551.2016.1232696.

[23] Johnson RL, Lehmann J, Olk DC, Neves EG, Thompson ML. 233-2012-Abundant and Stable Char Residues in Soils Implications for Soil Fertility and Carbon Sequestration.pdf 2012. doi:10.1021/es301107c.

[24] Wang C, Lu H, Dong D, Deng H, Strong PJ, Wang H, et al. Insight into the effects of biochar on manure composting: Evidence supporting the relationship between N2O emission and denitrifying community. Environ Sci Technol 2013;47:7341–9. doi:10.1021/es305293h.

[25] Yao Z, You S, Ge T, Wang CH. Biomass gasification for syngas and biochar co-production: Energy application and economic evaluation. Appl Energy 2018;209:43–55. doi:10.1016/j.apenergy.2017.10.077.

[26] Zhang C, Ho S, Chen W, Fu Y, Chang J, Bi X. Oxidative torrefaction of biomass nutshells : Evaluations of energy e ffi ciency as well as biochar transportation and storage. Appl Energy 2019;235:428–41. doi:10.1016/j.apenergy.2018.10.090.

[27] Khan FA, Pal N, Saeed SH. Review of solar photovoltaic and wind hybrid energy systems for sizing strategies optimization techniques and cost analysis methodologies. Renew Sustain Energy Rev 2018;92:937–47. doi:10.1016/j.rser.2018.04.107.

[28] Pérez-Uresti SI, Martín M, Jiménez-Gutiérrez A. Superstructure approach for the design of renewable-based utility plants. Comput Chem Eng 2019;123:371–88. doi:10.1016/j.compchemeng.2019.01.019.

[29] Li L, Liu P, Li Z, Wang X. A Multi-Objective Optimization Approach for Selection of Energy Storage Systems. Comput Chem Eng 2018. doi:https://doi.org/10.1016/j.compchemeng.2018.04.014.

[30] Zhou W, Lou C, Li Z, Lu L, Yang H. Current status of research on optimum sizing of stand-alone hybrid solar–wind power generation systems. Appl Energy 2010;87:380–9. doi:10.1016/J.APENERGY.2009.08.012.

[31] Chen S, Kumar A, Chin W, Chiu M, Wang X. Hydrogen value chain and fuel cells within hybrid renewable energy systems : Advanced operation and control strategies ☆. Appl Energy 2019;233–234:321–37. doi:10.1016/j.apenergy.2018.10.003.

[32] Zahraee SM, Khalaji Assadi M, Saidur R. Application of Artificial Intelligence Methods for Hybrid Energy System Optimization. Renew Sustain Energy Rev 2016;66:617–30. doi:10.1016/J.RSER.2016.08.028.

[33] Siddaiah R, Saini RP. A review on planning, configurations, modeling and optimization techniques of hybrid renewable energy systems for off grid applications. Renew Sustain Energy Rev 2016;58:376–96. doi:10.1016/j.rser.2015.12.281.

[34] Meng N, Xu Y, Huang G. A stochastic multi-objective optimization model for renewable energy structure adjustment management – A case study for the city of Dalian, China. Ecol Indic 2019;97:476–85. doi:10.1016/J.ECOLIND.2018.10.022.

[35] Gonzalez A, Riba J-R, Esteban B, Rius A. Environmental and cost optimal design of a biomass–Wind–PV electricity generation system. Renew Energy 2018;126:420–30. doi:10.1016/j.renene.2018.03.062.

[36] Ahmad J, Imran M, Khalid A, Iqbal W, Ashraf SR, Adnan M, et al. Techno economic analysis of a wind-photovoltaic-biomass hybrid renewable energy system for rural electrification: A case study of Kallar Kahar. Energy 2018;148:208–34. doi:10.1016/J.ENERGY.2018.01.133.

[37] Hocine A, Kouaissah N, Bettahar S, Benbouziane M. Optimizing renewable energy portfolios under uncertainty: A multi-segment fuzzy goal programming approach. Renew Energy 2018;129:540–52. doi:10.1016/j.renene.2018.06.013.

[38] Martín M, Grossmann IE. Optimal integration of renewable based processes for fuels and power production: Spain case study. Appl Energy 2018;213:595–610. doi:10.1016/J.APENERGY.2017.10.121.

[39] Chauhan A, Saini RP. Size optimization and demand response of a stand-alone integrated renewable energy system. Energy 2017;124:59–73. doi:10.1016/j.energy.2017.02.049.

[40] Chauhan A, Saini RP. Techno-economic optimization based approach for energy management of a stand-alone integrated renewable energy system for remote areas of India. Energy 2016;94:138–56. doi:10.1016/J.ENERGY.2015.10.136.

[41] Singh S, Singh M, Kaushik SC. Feasibility study of an islanded microgrid in rural area consisting of PV, wind, biomass and battery energy storage system. Energy Convers Manag 2016;128:178–90. doi:10.1016/j.enconman.2016.09.046.

[42] Sharifzadeh M, Sadeqzadeh M, Guo M, Borhani TN, Murthy Konda NVSN, Garcia MC, et al. The multi-scale challenges of biomass fast pyrolysis and bio-oil upgrading: Review of the state of art and future research directions. Prog Energy Combust Sci 2019;71:1–80. doi:10.1016/j.pecs.2018.10.006.

[43] Puig-Arnavat M, Hernández JA, Bruno JC, Coronas A. Artificial neural network models for biomass gasification in fluidized bed gasifiers. Biomass and Bioenergy 2013;49:279–89. doi:10.1016/J.BIOMBIOE.2012.12.012.

[44] Woolf D, Lehmann J, Fisher EM, Angenent LT. Biofuels from Pyrolysis in Perspective: Trade-offs between Energy Yields and Soil-Carbon Additions. Environ Sci Technol 2014;48:6492–9. doi:10.1021/es500474q.

[45] Field JL, Keske CMH, Birch GL, DeFoort MW, Cotrufo MF. Distributed biochar and bioenergy coproduction: a regionally specific case study of environmental benefits and economic impacts. Gcb Bioenergy 2013;5:177–91.

[46] Li W, Paul MC, Baig H, Siviter J, Montecucco A, Mallick TK, et al. A three-point-based electrical model and its application in a photovoltaic thermal hybrid roof-top system with crossed compound parabolic concentrator. Renew Energy 2019;130:400–15. doi:10.1016/j.renene.2018.06.021.

[47] De Soto W, Klein SA, Beckman WA. Improvement and validation of a model for photovoltaic array performance 2005. doi:10.1016/j.solener.2005.06.010.

[48] Ayang A, Wamkeue R, Ouhrouche M, Djongyang N, Essiane Salomé N, Pombe JK, et al. Maximum likelihood parameters estimation of single-diode model of photovoltaic generator. Renew Energy 2019;130:111–21. doi:10.1016/j.renene.2018.06.039.

[49] Tu T, Rajarathnam GP, Vassallo AM. Optimization of a stand-alone photovoltaic–wind–diesel–battery system with multi-layered demand scheduling. Renew Energy 2018. doi:10.1016/j.renene.2018.07.029.

[50] Wang X, Palazoglu A, El-Farra NH. Operation of residential hybrid renewable energy systems: Integrating forecasting, optimization and demand response. Proc Am Control Conf 2014:5043–8. doi:10.1109/ACC.2014.6859105.

[51] You S, Tong H, Armin-hoiland J, Wah Y, Wang C. Techno-economic and greenhouse gas savings assessment of decentralized biomass gasi fi cation for electrifying the rural areas of Indonesia. Appl Energy 2017;208:495–510. doi:10.1016/j.apenergy.2017.10.001.

[52] Mavromatidis G, Orehounig K, Carmeliet J. Design of distributed energy systems under uncertainty: A two-stage stochastic programming approach. Appl Energy 2018;222:932–50. doi:10.1016/j.apenergy.2018.04.019.

[53] Branke J, Deb K, Dierolf H, Osswald M. Finding Knees in Multi-objective Optimization 2004. https://www.iitk.ac.in/kangal/papers/k2004010.pdf (accessed October 10, 2018).

[54] Jing R, Wang M, Liang H, Wang X, Li N, Shah N, et al. Multi-objective optimization of a neighborhood-level urban energy network: Considering Game-theory inspired multi-benefit allocation constraints. Appl Energy 2018;231:534–48. doi:10.1016/J.APENERGY.2018.09.151.

[55] Philippine Standard Geographic Code | Philippine Statistics Authority 2018. http://nap.psa.gov.ph/activestats/psgc/province.asp?provCode=175900000 (accessed May 13, 2018).

[56] The lone sailor: a guide to Hambil Beach, Carabao Island, Romblon 2017. http://akosimerman.blogspot.sg/2017/09/travel-wise-guide-to-hambil-beach.html (accessed May 13, 2018).

[57] ECN Phyllis classification 2018. https://www.ecn.nl/phyllis2/Browse/Standard/ECN-Phyllis#sugarcane (accessed May 14, 2018).

[58] NASA. ASDC | Processing, archiving, and distributing Earth science data at the NASA Langley Research Center. 2018. https://eosweb.larc.nasa.gov/ (accessed May 13, 2018).

[59] NGCP. Operations - National Grid Corporation of the Philippines 2018. https://www.ngcp.ph/operations#situation (accessed December 24, 2018).